

Graph Topology Learning Under Privacy Constraints

Xiang Zhang, *Student Member, IEEE*, Qiao Wang, *Senior Member, IEEE*

Abstract—Graph learning, which aims to infer the underlying topology behind high dimension data, has attracted intense attention. In this study, we shed a new light on graph learning by considering a pragmatic scenario where data are privacy sensitive and located in separated clients (devices or organizations). The main difficulty in learning graphs in this scenario is that we cannot process all the data in a central server, because the data are not allowed to leave the local clients due to privacy concerns. The problem becomes more challenging when data of different clients are non-IID, since it is unreasonable to learn a global graph for heterogeneous data. To address these issues, we propose a novel framework in which a personalized graph for each client and a consensus graph are jointly learned in a federated fashion. Specifically, we commute model updates instead of raw data to the central server in the proposed federated algorithm. A provable convergence analysis shows that the algorithm enjoys $\mathcal{O}(1/T)$ convergence rate. To further enhance privacy, we design a differentially privacy algorithm to prevent the information of the raw data from being leaked when transferring model updates. A theoretical guidance is provided on how to ensure that the algorithm satisfies differential privacy. We also analyze the impact of differential privacy on the convergence of our algorithm. Finally, extensive experiments on both synthetic and real world data are carried out to validate the proposed models and algorithms. Experimental results illustrate that our framework is able to learn graphs effectively in the target scenario.

Index Terms—Graph learning, federated learning differential privacy, graph signal processing, privacy-preserving algorithm

I. INTRODUCTION

Graphs are powerful tools for characterizing structured data and widely used in numerous fields, e.g., machine learning [1], signal processing [2] and statistics [3], since vertices in graphs can represent data entities, and edges are used to describe hidden relationships between these entities [4]. Among these applications, it is crucial to construct some graphs, e.g., transport networks and social networks, using our prior knowledge. However, the prior graphs are not always available and may fail to capture the intrinsic relationships between data entities accurately [4]. An alternative way is to learn a graph directly from raw high dimensional data for some downstream tasks, e.g., graph neural network [5]. Inferring graph topology from data, also known as graph learning [6], has been a hot research topic in recent years. In addition to statistical models [3], [7], methods based on graph signal processing (GSP), an emerging research field [8], [9], attempt to learn graphs from perspective of signal processing. One of the most studied GSP models is based on smoothness assumption, under which signal values of two connected vertices with large edge weights tend to be similar

The authors are with the School of Information Science and Engineering, Southeast University, Nanjing 210096, China (e-mail: xiangzhang369@seu.edu.cn; qiaowang@seu.edu.cn).

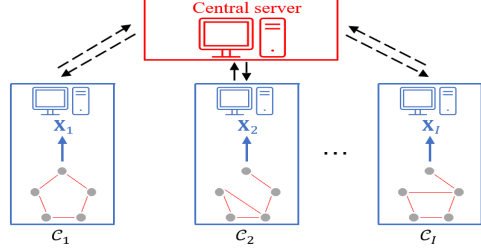


Fig. 1: The illustration of the target scenario. The clients $\mathcal{C}_1, \dots, \mathcal{C}_I$ store graphs signals $\mathbf{X}_1, \dots, \mathbf{X}_I$ generated from I distinct but related graphs. The data are not allowed to leave their clients due to privacy concerns. However, all clients can commute with a central server. We are required to learn graphs in this scenario.

[10]. Smoothness based graph learning models aim to learning graphs over which the signals are the smoothest [10], [11].

In this study, we shed a new light on graph learning by considering a pragmatic scenario. As shown in Fig.1, we assume that data are stored at different clients, e.g., devices and organizations, and privacy sensitive. Thus, they are forbidden to leave the local clients. A vivid example of this scenario is medical data. Suppose that some hospitals collect a set of brain fMRI data of autistic and normal people to learn the impact of autism on brain functional connectivity graphs. Due to the protection of patient privacy, the deliver of these data to an unreliable central server is not permitted. The data silos prevent us from learning reliable graphs using data from all clients, resulting in poor learning performance. On the other hand, the local data may come from different but related graphs defined on the same node sets, resulting in non-IID data. We still use brain fMRI data as an example. The brain functional connection changes due to the impact of autism, and the resulting graph signals are naturally not from the same distribution. Learning graphs from heterogeneous data is also a challenging problem. In summary, the challenges of the problem we focus on are as follows. (i) We need to learn graphs by leveraging information from data stored at multiple local clients under privacy constraints. The data can only be stored and processed in local clients. (ii) We are required to learn meaningful graphs using heterogeneous data.

Privacy constraints aside, if we only care about learning graphs using heterogeneous data, the problem boils down to multiple graph learning (MGL). The crux of MGL is to design a regularizer that captures relationships across the graphs. Miscellaneous researches have been conducted on MGL, which can be roughly divided into two categories, i.e., statistical models and GSP based models. Different from statistical models that learn precision matrices [12]–[16], our model focus on learning valid Laplacian matrices, which is based on

GSP models. The GSP based MGL models also consist of two categories, i.e., models based on stationary assumptions [17], [18] and models based on smoothness assumptions. The problem of interest in this study belongs to the second category. The most studied smoothness based MGL models are those that learn time-varying graphs [19], [20]. These models only exploit the relationships between temporally adjacent graphs. Recent studies [21], [22] leverage Gram matrices to describe complex topological patterns between graphs. However, none of these models attempt to learn multiple graphs under privacy constraints, which is the main focus of this study.

As for privacy constraints, federated learning (FL) [23] is an increasingly interesting tool to address the challenge. FL involves learning statistical models based on datasets that are distributed across multiple devices or institutions [24]. A major feature of FL is that the raw data are stored and processed locally due to privacy concerns [24], [25], which is the same as the issues we care about in this study. In FL, model updates are exchanged instead of raw data, and hence data privacy is preserved to a certain extent [24]. However, standard FL framework aims to learn a single global model for all data [26], which is not suitable for our scenario. As mentioned in the second challenge, graph topology varies from client to client, leading to heterogeneous data. Thus, it is not reasonable to learn a single global graph for all clients. A widely-used method to handle data heterogeneity in FL is the personalized federated learning (PFL) [27]. The philosophy behind PFL is that we learn a personalized model for each client that matches the local data distribution. Some techniques for adapting global models for individual clients include transfer learning [28], multi-task learning [29], [30] and meta-learning [31]. In this study, we construct our formulation starting with multi-task learning based PFL. Specifically, we jointly learn graphs for all client by exploiting some underlying relationships between them under federated learning framework.

Although classic FL framework takes a step toward preserving data privacy (exchanging model updates instead of raw data), transmitting model updates may still leak some sensitive information of private data [32]. To further enhance data privacy, some privacy-preserving machine learning tools are incorporated into federated learning framework [33], [34], e.g., differential privacy (DP) [35]. DP provides an efficient tool to define individual privacy. Simply put, if an algorithm is differentially private, the estimated model should be indistinguishable whether or not a particular user's data is considered. A popular approach to achieve DP is randomly adding noise to the intermediate output at each iteration [36]. Compared with other privacy-preserving tools, DP provides strong information theoretic guarantees, see [37] for a thorough review. In this study, we are desired to design an graph learning scheme satisfying DP. To the best of our knowledge, none of the previous models have addressed this issue.

The contributions of this paper can be concluded as follows.

Firstly, we propose a multiple graph learning framework under smoothness assumption. In our framework, graphs of different clients are connected via a consensus graph. To be specific, we assume that there exist some common structures in the graphs of all clients. This assumption enjoys a wide

range of real-world applications, and one of them is single cell RNA sequencing (scRNA-seq) dataset. Generally speaking, the datasets collected in a single experiment often contain cells belonging to different cellular subtypes [38]. The graphs of these cells share some common structures since they belong to the different clusters originated from the same tissue. Another example is the multimedia data that are collected from various input channels, e.g., photos of the same objects taken from different angles. These photos share the same semantic details since they are from the same objects [39]. In light of these observations, we design a regularizer based on the assumption that all local graphs are similar with a consensus graph. The consensus graph should be sparse such that the noise generated by different views can be alleviated [40]. Using the regularizer, we jointly learn the local graphs and the consensus graph. The formulation has an merit that the consensus graph can capture the common structures across these local graphs, while the local graphs can retain heterogeneity of each local dataset.

Secondly, we propose an algorithm that learns graphs in a federated fashion. In this algorithm, the raw data are stored and processed on the local clients, which protects the data privacy to a certain extent. To "borrow" information from the data of other clients, we commute model updates, rather than raw data, to the central server to exchange information. All graphs, including the consensus graph, are jointly learned without delivering raw data to the central server. A provable convergence analysis of the proposed algorithm is provided, and the results demonstrate that our algorithm reaches $\mathcal{O}(1/T)$ convergence rate, where T is the number of iterations.

Thirdly, to further enhance privacy during learning process, we design a differentially private algorithm to prevent information of raw data from being leaked when commuting model updates. Specifically, we provide a provable theoretical guidance on how to ensure that the transfer of data satisfies DP. Furthermore, we also analyze the convergence of the proposed differentially private algorithm.

Finally, we carry out extensive experiments on synthetic and real world data to validate our framework. Experimental results illustrate that our framework can effectively learn a graph for each client even under privacy constraints.

Organization: The rest of this paper is organized as follows. We first introduce the background information in Section II-A. We propose our graph learning model under federated learning framework in Section III. Federated graph learning algorithm with DP is introduced in IV. Experiments are carried out to validate our model in Section V. Finally, some concluding remarks are presented in Section VI.

Notations: Throughout this paper, vectors and matrices are written in bold lowercase and bold uppercase letters respectively. Sets are denoted by calligraphic capital letters. Moreover, $\mathbf{y}_{[i]}$ and $\mathbf{Y}_{[ij]}$ denote the i -th and (i, j) entry of \mathbf{y} and \mathbf{Y} respectively. The ℓ_1 , ℓ_2 and Frobenius norm are denoted as $\|\cdot\|_1$, $\|\cdot\|_2$ and $\|\cdot\|_F$. The notations \circ , \dagger , $\text{Tr}(\cdot)$ and $\text{Pr}(\cdot)$ mean Hadamard product, pseudo inverse, trace operator and taking probability. $\text{diag}(\mathbf{y})$, $\text{diag}(\mathbf{Y})$ and $\text{diag}_0(\mathbf{Y})$ stand for converting a vector \mathbf{y} to a diagonal matrix, converting the diagonal elements of \mathbf{Y} to a vector and setting the diagonal entries of \mathbf{Y} to 0. Furthermore, $\mathbf{y} \geq 0$ and $\mathbf{Y} \geq 0$ mean that all

elements of \mathbf{y} and \mathbf{Y} are greater than zero. The vectors $\mathbf{1}, \mathbf{0}$ and matrix \mathbf{I} represent column vector of ones, zeros and identity matrix. The $Gauss(\mathbf{y}, \mathbf{Y})$ denotes Gaussian distribution with mean \mathbf{y} and covariance \mathbf{Y} . For a set \mathcal{Y} , $\text{conv}[\mathcal{Y}]$ denotes the affine and convex hulls of \mathcal{Y} . Finally, \mathbb{R} denotes the set of real values. The superscript of \mathbb{R} denotes dimensions of vector (matrices) and subscripts $+$ denotes nonnegative constraint.

II. BACKGROUND AND PROBLEM STATEMENT

A. GSP Background

We only focus on undirected graphs with nonnegative weights and no self-loops. For such a graph \mathcal{G} with d vertices, its adjacency matrix \mathbf{W} is a $d \times d$ symmetric matrix with zero diagonal entries and nonnegative off-diagonal entries. The Laplacian matrix of \mathcal{G} is another important matrix, which is defined as $\mathbf{L} = \mathbf{D} - \mathbf{W}$ [2]. The degree matrix \mathbf{D} is a $d \times d$ diagonal matrix with $\mathbf{D}_{[ii]} = \sum_{j=1}^d \mathbf{W}_{[ij]}$. We use \mathbf{W} and \mathbf{L} to represent the topology of \mathcal{G} since they have a one-to-one relationship. A graph signal $\mathbf{x} = [\mathbf{x}_{[1]}, \dots, \mathbf{x}_{[d]}]^\top$ of graph \mathcal{G} means that every dimension of \mathbf{x} is regarded as a node in \mathcal{G} . Furthermore, edges of \mathcal{G} describe the relationships between dimensions of \mathbf{x} , and weights quantify the “closeness” of these relationships. Since our model is based on smoothness assumption, we provide the definition of smoothness as follows.

Definition 1. (Smoothness, [10]). *Given a graph signal \mathbf{x} and the Laplacian matrix \mathbf{L} of graph \mathcal{G} , the smoothness of \mathbf{x} over \mathcal{G} is defined as*

$$\mathbf{x}^\top \mathbf{L} \mathbf{x} = \frac{1}{2} \sum_{i,j} \mathbf{W}_{[ij]} (\mathbf{x}_{[i]} - \mathbf{x}_{[j]})^2. \quad (1)$$

The smaller value of (1) is, the smoother the signal over \mathcal{G} . From the definition of smoothness, if a signal is smooth over \mathcal{G} , the values of two dimensions connected with large edges weight of \mathcal{G} should be similar.

B. Smoothness Based Graph Learning

Given N observations $\mathbf{X} = [\mathbf{x}_1, \dots, \mathbf{x}_N]$, smoothness based graph learning is aimed to infer the hidden graph topology, i.e., \mathbf{W} or \mathbf{L} , using the assumption that graph signals are smoothest over the graphs to learn. Formally, the problem is written as

$$\min_{\mathbf{L} \in \mathcal{L}} \sum_{i=1}^N \frac{2}{N} \mathbf{x}_i^\top \mathbf{L} \mathbf{x}_i + r(\mathbf{L}), \quad (2)$$

where $r(\mathbf{L})$ is a regularization term of \mathbf{L} to obtain some desired property of graphs, e.g., sparsity. Moreover, \mathcal{L} is the set containing all Laplacian matrices

$$\mathcal{L} \triangleq \{\mathbf{L} : \mathbf{L} = \mathbf{L}^\top, \mathbf{L}\mathbf{1} = \mathbf{0}, \mathbf{L}_{[ij]} \leq 0 \text{ for } i \neq j\}. \quad (3)$$

In this study, we follow [11] and select $r(\mathbf{L})$ as $-\alpha \mathbf{1}^\top \log(\text{diag}(\mathbf{L})) + \beta \|\text{diag}_0(\mathbf{L})\|_F^2$, where α and β are predefined parameters. The first term of $r(\mathbf{L})$ controls degrees of each node, while the second term controls sparsity of edges [11]. With $r(\mathbf{L})$, (2) can also be written in the form of adjacent matrix \mathbf{W} [11], i.e.,

$$\min_{\mathbf{W} \in \mathcal{A}} (1/N) \|\mathbf{W} \circ \mathbf{Z}\|_1 - \alpha \mathbf{1}^\top \log(\mathbf{W}\mathbf{1}) + \beta \|\mathbf{W}\|_F^2, \quad (4)$$

where \mathcal{A} is the set defined as

$$\mathcal{A} = \{\mathbf{W} : \mathbf{W} \in \mathbb{R}_+^{d \times d}, \mathbf{W} = \mathbf{W}^\top, \text{diag}(\mathbf{W}) = \mathbf{0}\}. \quad (5)$$

Furthermore, $\mathbf{Z} \in \mathbb{R}^{d \times d}$ in (4) is a pairwise distance matrix. Let's denote $\mathbf{X}^\top = [\tilde{\mathbf{x}}_1, \dots, \tilde{\mathbf{x}}_d]$, where $\tilde{\mathbf{x}}_i \in \mathbb{R}^N$ is the i -th row vector of \mathbf{X} . The (i, j) entry of \mathbf{Z} is equivalent to

$$\mathbf{Z}_{[ij]} = \|\tilde{\mathbf{x}}_i - \tilde{\mathbf{x}}_j\|_2^2. \quad (6)$$

Since \mathbf{W} is a symmetric matrix with diagonal entries equal to 0, the number of free variables of \mathbf{W} is actually $\frac{d(d-1)}{2}$ [11]. For simplicity, we let $p \triangleq \frac{d(d-1)}{2}$ and define a vector $\mathbf{w} \in \mathbb{R}^p$ whose entries are the upper triangle variables of \mathbf{W} . The vector \mathbf{w} also has one-to-one relationship with \mathcal{G} . With the definition of \mathbf{w} , (4) can be rewritten as [11]

$$\min_{\mathbf{w} \geq 0} (2/N) \mathbf{z}^\top \mathbf{w} - \alpha \mathbf{1}^\top \log(\mathbf{Sw}) + 2\beta \|\mathbf{w}\|_2^2, \quad (7)$$

where \mathbf{S} is a linear operator satisfying $\mathbf{Sw} = \mathbf{W}\mathbf{1}$, and \mathbf{z} is the vector form of the upper triangle elements in \mathbf{Z} . Note that \mathbf{z} is calculated using data matrix \mathbf{X} , and hence \mathbf{z} is also regarded as a data vector in later sections.

C. Problem Statement

As shown in Fig.1, suppose there are I clients $\mathcal{C}_1, \dots, \mathcal{C}_I$, and the i -th client stores the signals $\mathbf{X}_i \in \mathbb{R}^{d \times N_i}$ generated from the local graph \mathcal{G}_i , where N_i is the data size of the i -th dataset. The graphs of different clients are assumed to be distinct but related, and defined over the same node set. The graph signals \mathbf{X}_i are smooth over the graph \mathcal{G}_i , and are forbidden from leaving the corresponding clients due to privacy concerns. However, the clients can communicate with a central server. We are required to learn $\mathcal{G}_1, \dots, \mathcal{G}_I$ under privacy constraints and with heterogeneous data $\mathbf{X}_1, \dots, \mathbf{X}_I$.

III. FEDERATED GRAPH LEARNING

A. Basic formulation

In our formulation, we assume there exists a consensus graph that captures the common structures across graphs of all clients. We learn the local graphs $\mathcal{G}_1, \dots, \mathcal{G}_I$ and the consensus graph \mathcal{G}_{con} jointly via

$$\begin{aligned} \min_{\mathbf{w}_i \in \mathcal{W}, \mathbf{w}_{\text{con}}} & \sum_{i=1}^I \underbrace{\frac{1}{N_i} \sum_{n=1}^{N_i} 2\mathbf{z}_{i,n}^\top \mathbf{w}_i - \alpha \mathbf{1}^\top \log(\mathbf{Sw}_i) + 2\beta \|\mathbf{w}_i\|_2^2}_{g_i(\mathbf{w}_i)} \\ & + \rho \sum_{i=1}^I \|\mathbf{w}_i - \mathbf{w}_{\text{con}}\|_2 + \lambda \|\mathbf{w}_{\text{con}}\|_1, \end{aligned} \quad (8)$$

where $\mathbf{z}_{i,n}$ is the pair-wise distance vector of n -th data \mathbf{x}_n in i -th client and $\mathcal{W} \triangleq \{\mathbf{w} : \mathbf{w} \geq 0\}$. Moreover, \mathbf{w}_i and \mathbf{w}_{con} denote the vectorized adjacency matrices of \mathcal{G}_i and \mathcal{G}_{con} respectively. In this model, $g_i(\mathbf{w}_i)$ represents the classic smoothness based graph learning for each local client. The term $\|\mathbf{w}_i - \mathbf{w}_{\text{con}}\|_2$ is used to measure the difference between \mathbf{w}_i and \mathbf{w}_{con} , and ρ is a parameter that controls the global weight of the term describing relationships between graphs. We add the last term of (8) because the consensus graph is expected to be sparse, which can remove noisy edges. The parameter λ controls the density of \mathbf{w}_{con} . Observe that the hyper parameters of (8) are α, β, ρ and λ . However, as stated in [11], there exists a scaling effect when we tune α with respect to β . We can fix α as a constant and search only β for the desired edge density. Therefore, the free parameters of our

problem are β , ρ and λ . In the experimental section, we will show that λ can hardly affect the local graphs and is hence easy to tune. Finally, we use grid search for the best β and ρ . The proposed formulation (8) enjoys the following advantages. From the view of graph learning, the formulation provides a way to jointly learn graphs of different clients. Compared with learning graphs independently, our formulation benefits from borrowing information from other datasets, which may boost learning performance. From the perspective of federated learning, we learn a personalized graph for each client, which can alleviate the bias of learning a single global graph in the case of data heterogeneity. Furthermore, we also learn a consensus graph that reflects the global information.

We choose ℓ_2 norm to measure the difference between \mathbf{w}_i and \mathbf{w}_{con} for the reason that we can adaptively adjust the weight of similarity between \mathbf{w}_i and \mathbf{w}_{con} . We will next explain in detail. Inspired by the inverse distance weighting scheme [41], we write down the Lagrange function of (8) as

$$\min_{\mathbf{V}} \rho \sum_{i=1}^I \|\mathbf{w}_i - \mathbf{w}_{\text{con}}\|_2 + G(\mathbf{V}) + L(\mathbf{V}, \Lambda), \quad (9)$$

where $G(\mathbf{V}) = \sum_{i=1}^I g_i(\mathbf{w}_i) + \lambda \|\mathbf{w}_{\text{con}}\|_1$ and \mathbf{V} is the variable composed of \mathbf{w}_i and \mathbf{w}_{con} . Moreover, $L(\mathbf{V}, \Lambda)$ serves as a proxy for the constraints to \mathbf{V} , and Λ is the Lagrange multiplier. Taking the derivative of (9) w.r.t. \mathbf{V} and setting it to zero, we obtain

$$\frac{\rho}{2} \sum_{i=1}^I \gamma_i \frac{\partial \|\mathbf{w}_i - \mathbf{w}_{\text{con}}\|_2^2}{\partial \mathbf{V}} + \frac{\partial G(\mathbf{V})}{\partial \mathbf{V}} + \frac{\partial L(\mathbf{V}, \Lambda)}{\partial \mathbf{V}} = \mathbf{0}, \quad (10)$$

where

$$\gamma_i = 1/\|\mathbf{w}_i - \mathbf{w}_{\text{con}}\|_2. \quad (11)$$

We can find that γ_i is dependent on \mathbf{V} , and (10) cannot be directly solved. However, if γ_i is set to be stationary, (10) is equivalent to solving the following problem

$$\min_{\mathbf{w}_i \in \mathcal{W}, \mathbf{w}_{\text{con}}} \sum_{i=1}^I g_i(\mathbf{w}_i) + \frac{\rho \gamma_i}{2} \|\mathbf{w}_i - \mathbf{w}_{\text{con}}\|_2^2 + \lambda \|\mathbf{w}_{\text{con}}\|_1. \quad (12)$$

The solved \mathbf{w}_i and \mathbf{w}_{con} from (12) can be in turn used to update γ_i in (11). Therefore, we can optimize the problem (8) in an alternative way, which will be introduced in detail in next subsection. From the update of γ_i , we can automatically adjust the weight of difference between \mathbf{w}_i and \mathbf{w}_{con} . For those \mathbf{w}_i is close to \mathbf{w}_{con} , a larger γ_i is assigned to the corresponding term, increasing the contribution of the i -th graph to the consensus graph.

B. Algorithm

We propose a algorithm in a federated fashion to solve (8). In our algorithm, we alternatively update \mathbf{w}_i , \mathbf{w}_{con} and γ_i , and all data are processed locally. Our algorithm consists of two steps, i.e., updating \mathbf{w}_i in the corresponding local client and updating $\gamma = [\gamma_1, \dots, \gamma_I]^\top$, \mathbf{w}_{con} in a third-party centeral server. The complete algorithm flow is shown in Algorithm 1.

Updating \mathbf{w}_i in local clients: This part of the update corresponds to lines 3-8 in Algorithm 1. In the t -th outer loop, the subproblem of i -th local dataset is

$$\mathbf{w}_i^{t+1} = \underset{\mathbf{w}_i \in \mathcal{W}}{\text{argmin}} \frac{1}{N_i} \sum_{n=1}^{N_i} 2\mathbf{z}_{i,n}^\top \mathbf{w}_i - \alpha \mathbf{1}^\top \log(\mathbf{S}\mathbf{w}_i) + 2\beta \|\mathbf{w}_i\|_2^2$$

$$+ \frac{\rho \gamma_i^t}{2} \|\mathbf{w}_i - \mathbf{w}_{\text{con}}^t\|_2^2. \quad (13)$$

We use accelerate projection gradient descent algorithm to update \mathbf{w}_i of each client. At the beginning of the t -th iteration, the client i first receives consensus graph $\mathbf{w}_{\text{con}}^t$ and γ_i^t from the central server and initializes $\mathbf{w}_i^{t,0} = \mathbf{w}_i^{t-1, K_i^{t-1}}$ and $\mathbf{w}_i^{t,-1} = \mathbf{w}_i^{t-1, K_i^{t-1}-1}$, where K_i^t denotes the number of iterations we run in client i of outer iterations t . Furthermore, $\mathbf{w}_i^{t,k}$ means the updated graph in outer iterations t and inner iteration k of the i -th client. Using the accelerate projection gradient descent, we update the i -th local graph K_i^t times by

$$\mathbf{w}_{i,\text{ex}}^{t,k} = \mathbf{w}_i^{t,k} + \xi (\mathbf{w}_i^{t,k} - \mathbf{w}_i^{t,k-1}) \quad (14)$$

$$\check{\mathbf{w}}_i^{t,k+1} = \mathbf{w}_{i,\text{ex}}^{t,k} - \eta_w \left(\nabla g_i(\mathbf{w}_{i,\text{ex}}^{t,k}) + \rho \gamma_i^t (\mathbf{w}_{i,\text{ex}}^{t,k} - \mathbf{w}_{\text{con}}^t) \right) \quad (15)$$

$$\mathbf{w}_i^{t,k+1} = \text{Proj}_{\mathcal{W}} (\check{\mathbf{w}}_i^{t,k+1}), \quad (16)$$

where $\xi \in [0, 1]$ is the momentum weight. In (15), $\nabla g_i(\mathbf{w})$ is calculated as $(2/N_i) \sum_{n=1}^{N_i} \mathbf{z}_{i,n} - \alpha \mathbf{S}^\top (\mathbf{S}\mathbf{w})^{(-1)} + 4\beta \mathbf{w}_i$. Moreover, η_w is the stepsize, and its selection will be introduced in the next subsection. The operator $\text{Proj}_{\mathcal{W}}(\cdot)$ means projecting varibales to the set \mathcal{W} . When the update of \mathbf{w}_i finishes, the client i sends \mathbf{w}_i^{t+1} to the central server. Note that the update of the i -th graph \mathbf{w}_i is inexact in the t -th iteration since we only run the above updates for K_i^t times without converging. The reason why we use inexact updates is that we hope to update all graphs synchronously. Due to system heterogeneity, the time each client takes to update \mathbf{w}_i until it converges may vary widely. Therefore, it will take more time if the central server waits for all clients to update their graphs until convergence. We will prove that the inexact updates of \mathbf{w}_i do not affect the convergence of the algorithm.

Updating γ and \mathbf{w}_{con} in the center server: After the central server receives all updated local graphs, we first update $\mathbf{w}_{\text{con}}^{t+1}$ by solving the following problem

$$\mathbf{w}_{\text{con}}^{t+1} = \underset{\mathbf{w}_{\text{con}}}{\text{argmin}} \sum_{i=1}^I \frac{\rho \gamma_i^t}{2} \|\mathbf{w}_i^{t+1} - \mathbf{w}_{\text{con}}\|_2^2 + \lambda \|\mathbf{w}_{\text{con}}\|_1. \quad (17)$$

The problem can be further written as

$$\mathbf{w}_{\text{con}}^{t+1} = \underset{\mathbf{w}_{\text{con}}}{\text{argmin}} \frac{1}{2} \left\| \mathbf{w}_{\text{con}} - \frac{\sum_{i=1}^I \gamma_i^t \mathbf{w}_i^{t+1}}{\sum_{i=1}^I \gamma_i^t} \right\|_2^2 + \frac{\lambda}{\rho \sum_{i=1}^I \gamma_i^t} \|\mathbf{w}_{\text{con}}\|_1. \quad (18)$$

It is easy to check that (18) is the proximal operator of ℓ_1 norm. If we define $C_\gamma^t = \sum_{i=1}^I \gamma_i^t$ and let $\mu = \frac{\lambda}{C_\gamma^t \rho}$, we finally obtain the update as

$$\mathbf{w}_{\text{con}}^{t+1} = \text{prox}_{\mu \|\cdot\|_1} \left(\frac{\sum_{i=1}^I \gamma_i^t \mathbf{w}_i^{t+1}}{C_\gamma^t} \right), \quad (19)$$

where $\text{prox}_{\mu \|\cdot\|_1}(\cdot)$ is the proximal operator of ℓ_1 norm.

After obtaining $\mathbf{w}_{\text{con}}^{t+1}$, we adaptively update γ_i^{t+1} using

$$\gamma_i^{t+1} = \frac{1}{\|\mathbf{w}_i^{t+1} - \mathbf{w}_{\text{con}}^{t+1}\|_2 + \epsilon_\gamma}, \quad \text{for } i = 1, \dots, I, \quad (20)$$

where ϵ_γ is a small enough value. Finally, we send $\mathbf{w}_{\text{con}}^{t+1}$ and γ_i^{t+1} back to the i -th client.

Algorithm 1 Federated graph learning

Input:

$\alpha, \beta, \rho, \xi, \lambda$ signals $\mathbf{X}_1, \dots, \mathbf{X}_I$
1: **Initialize** $\mathbf{w}_{\text{con}}^0, \gamma_i^0 = 1/I$ and $\mathbf{w}_i^{(-1,0)} = \mathbf{w}_i^{(-1,-1)}$ for
 $i = 1, \dots, I$
2: **for** $t = 0, \dots, T - 1$ **do**
3: **// Update $\mathbf{w}_1, \dots, \mathbf{w}_I$ in parallel in local clients**
4: Receive consensus graph and $\gamma_i^t, \mathbf{w}_{\text{con}}^t$ from central
server
5: Initialize $\mathbf{w}_i^{t,0} = \mathbf{w}_i^{t-1, K_i^{t-1}}$ and $\mathbf{w}_i^{t,-1} = \mathbf{w}_i^{t-1, K_i^{t-1}-1}$
6: **for** $k = 0, \dots, K_i^t - 1$ **do**
7: Update $\mathbf{w}_i^{t,k+1}$ using (14) - (16)
8: **end for**
9: Let $\mathbf{w}_i^{t+1} = \mathbf{w}_i^{(t, K_i^t)}$ and send \mathbf{w}_i^{t+1} to central server
10: **// Update $\mathbf{w}_{\text{con}}^t$ in central server**
11: Update $\mathbf{w}_{\text{con}}^{t+1}$ using (19)
12: Update γ_i^{t+1} using (20)
13: Send $\mathbf{w}_{\text{con}}^{t+1}$ and γ_i^{t+1} to the i -th client
14: **end for**
15: **return** $\mathbf{w}_1^T, \dots, \mathbf{w}_I^T$ and $\mathbf{w}_{\text{con}}^T$

C. Convergence analysis

In this section, we provide the convergence analysis of our proposed algorithm. Some assumptions essential to the theoretical analysis are first made.

Assumption 1. All received data are bounded, i.e., there exists a constant $B_z > 0$ such that $\|\mathbf{z}_{i,n}\|_2 \leq B_z$ for all $i = 1, \dots, I$, $n = 1, \dots, N_i$.

Assumption 2. The updated results in the search space are bounded, i.e., for any \mathbf{a} and $\mathbf{b} \in \mathcal{W}$, $\|\mathbf{a} - \mathbf{b}\|_2 \leq B_r$. Furthermore, for any updated \mathbf{a} and $\mathbf{b} \in \widetilde{\mathcal{W}}$, $\|\mathbf{a} - \mathbf{b}\|_2 \leq B_w$, where $\widetilde{\mathcal{W}} = \text{conv}[\cup_{0 \leq \xi \leq 1} \{\mathbf{a} + \xi(\mathbf{a} - \mathbf{b}) \mid \mathbf{a}, \mathbf{b} \in \mathcal{W}\}]$ is the extended feasible set.

Assumption 3. The (constant) stepsizes satisfy that $\eta_w \leq \min\{1/L_i, i, \dots, I\}$, where L_i is the Lipschitz constant of the gradient of f_i . We will introduce L_i in detail later.

Without loss of generality, Assumption 1 holds true naturally in real-world applications. Assumption 2 is common in the convergence analysis of constrained optimization problems. The choice of η_w as stated in Assumption 3 is necessary in gradient descent type algorithm [42]. Next, let's take a closer look at the properties of the objective function of (8).

Proposition 1. Under Assumption 1-3, for a given γ , the objective function $f_i(\mathbf{w}_i, \mathbf{w}_{\text{con}}) = \frac{1}{N_i} \sum_{n=1}^{N_i} 2\mathbf{z}_{i,n}^\top \mathbf{w}_i - \alpha \mathbf{1}^\top \log(\mathbf{S}\mathbf{w}_i) + 2\beta \|\mathbf{w}_i\|_2^2 + \frac{\rho\gamma_i}{2} \|\mathbf{w}_i - \mathbf{w}_{\text{con}}\|_2^2$ is $\rho\gamma_i$ -Lipschitz smooth w.r.t. \mathbf{w}_{con} and L_i -Lipschitz smooth w.r.t. \mathbf{w}_i on $\widetilde{\mathcal{W}}$, where $L_i = 4\beta + 2\alpha(d-1)/\text{deg}_{\min}^2 + \rho\gamma_i$ and deg_{\min} is the smallest degree of all graphs in the search space. Furthermore, the partial gradient of f_i w.r.t \mathbf{w}_i is also bounded by a constant $B_g = 2B_z + (4\beta + \rho\gamma_i)B_w + \alpha\sqrt{2d(d-1)}/\text{deg}_{\min}$.

Proof: See Appendix A for more details. ■

The convergence of our algorithm is as follows.

Theorem 1. Suppose that Assumptions 1-3 hold, the sequences $\mathbf{w}_i^t, \mathbf{w}_{\text{con}}^t$ generated from our algorithm satisfy

$$\frac{1}{T} \sum_{t=0}^{T-2} \left(\sum_{i=1}^I \|\mathbf{w}_i^{t+1} - \mathbf{w}_i^t\|_2^2 \right) \leq \frac{C_1}{T} \quad (21)$$

$$\frac{1}{T} \sum_{t=0}^{T-1} \|\mathbf{w}_{\text{con}}^{t+1} - \mathbf{w}_{\text{con}}^t\|_2^2 \leq \frac{C_2}{T}, \quad (22)$$

where

$$C_1 = \frac{2\Delta\eta_w}{1 - \xi^2}, \quad C_2 = \frac{2B_r\Delta}{\rho I},$$

$$\Delta = \sum_{i=1}^I f_i(\mathbf{w}_i^0, \mathbf{w}_{\text{con}}^0) - f_i^{\min} + \lambda\sqrt{p}B_r. \quad (23)$$

In (23), f_i^{\min} denotes the minimum of f_i .

Proof: See Appendix B for more details. ■

The Theorem indicates that our algorithm enjoys convergence rate of $\mathcal{O}(1/T)$ for both \mathbf{w}_i and \mathbf{w}_{con} .

D. Privacy analysis

In our algorithm, we update $\mathbf{w}_1, \dots, \mathbf{w}_I$ locally with only their own private data. Observe that the transmitted data between clients and the central server are the learned graphs. There is no direct exchange of private data during algorithm execution. Therefore, data privacy can be preserved to a certain extent. However, transmitting model updates can nonetheless reveal sensitive information to the attackers [24]. Thus, a more strong privacy-preserving mechanism is required to prevent sensitive information leakage in our federated graph learning problem, which will be introduced in next section.

IV. FEDERATE GRAPH LEARNING WITH DIFFERENTIAL PRIVACY

A. Basic Formulation

We assume that there exists an adversary who can observe all information commuted between clients and central servers, but cannot access the internal memory of each local client. We hope that the adversary cannot infer much information about any individual data of any local client from the eavesdropped model update information. In this scenario, we need to implement privacy protection mechanisms for the output of all clients. Before further discussions, we first need to formally define individual privacy. In this study, we exploit differential privacy (DP) [43] to measure how much information about any individual data point of a dataset is contained in the output of an algorithm.

Definition 2. (ϵ, δ) -DP ([43]) Let $\epsilon > 0, \delta \geq 0$, a randomized mechanism M is called (ϵ, δ) -differentially private if for any two neighboring datasets \mathcal{D}^1 and \mathcal{D}^2 , and for any subset $\mathcal{S} \subseteq \mathcal{Y}$, where \mathcal{Y} is the set of all possible outputs, it holds

$$\Pr[M(\mathcal{D}^1) \in \mathcal{S}] \leq e^\epsilon \Pr[M(\mathcal{D}^2) \in \mathcal{S}] + \delta. \quad (24)$$

In this definition, two datasets \mathcal{D}^1 and \mathcal{D}^2 being neighboring means that \mathcal{D}^1 can be obtained from \mathcal{D}^2 by adding or subtracting one single record of data [44]. The randomized

mechanism M can be regarded as any algorithm that takes a dataset as input, and the output can be model updates as mentioned before. The Definition 2 provides a theoretical tool to measure the level of privacy through (ϵ, δ) , and smaller (ϵ, δ) corresponds to increased privacy. For those small (ϵ, δ) , it is difficult for us to tell the difference between the output of the randomized mechanism M on two adjacent datasets. Therefore, the eavesdropper can hardly learn the information of any individual data point of the datasets. The core problem then becomes that, given (ϵ, δ) , how to design M so that the outputs satisfy (ϵ, δ) -DP. In our federated graph learning problem, each client i runs the mechanism $M_i(\mathcal{D}_i)$ on the local dataset \mathcal{D}_i and sends its outputs to the central server. Therefore, we hope that the randomized mechanisms $M_i(\mathcal{D}_i)$ for all clients to satisfy (ϵ, δ) -DP simultaneously. In the next section, the detailed design of M_i will be provided.

B. Algorithm

To ensure that the mechanism M satisfies (ϵ, δ) -DP, a widely used method is to add noise (uncertainty) to the released data, which can mask the contribution of any individual user [23]. In this study, we leverage Gaussian mechanism to build our privacy-preserving algorithm. Specifically, we add Gaussian noise $\mathbf{s} \sim \text{Gauss}(0, \sigma)^p \in \mathbb{R}^p$ to the gradient information of (15) before we release the model updates. The framework of the algorithm with PD is based on Algorithm 1, and the modification is as follows.

Updating \mathbf{w}_i in local clients: In the i -th client, we first update \mathbf{w}_i $K_i^t - 1$ times following the same way as line 7 in Algorithm 1. In the K_i^t -th iteration, we add Gaussian noise to the gradient $\nabla g_i(\mathbf{w}_{i,\text{ex}}^{t,k})$ since it contains the information of raw data. The update is

$$\mathbf{w}_{i,\text{ex}}^{t,K_i^t-1} = \mathbf{w}_i^{t,K_i^t-1} + \xi \left(\mathbf{w}_i^{t,K_i^t-1} - \mathbf{w}_i^{t,K_i^t-2} \right) \quad (25)$$

$$\begin{aligned} \tilde{\mathbf{w}}_i^{t,K_i^t} = & \mathbf{w}_{i,\text{ex}}^{t,K_i^t-1} - \eta_w \left(\nabla g_i \left(\mathbf{w}_{i,\text{ex}}^{t,K_i^t-1} \right) + \mathbf{s}_i \right. \\ & \left. + \rho \gamma_i^t \left(\mathbf{w}_{i,\text{ex}}^{t,K_i^t-1} - \mathbf{w}_{\text{con}}^t \right) \right) \end{aligned} \quad (26)$$

$$\mathbf{w}_i^{t,K_i^t} = \text{Proj}_{\mathcal{W}} \left(\tilde{\mathbf{w}}_i^{t,K_i^t} \right), \quad (27)$$

where $\mathbf{s}_i^t \sim (0, \sigma_i^t)^p \in \mathbb{R}^p$ is the Gaussian noise added in the t -th iteration of the i -th client. We then set $\tilde{\mathbf{w}}_i^{t+1} = \tilde{\mathbf{w}}_i^{t,K_i^t}$, and send $\tilde{\mathbf{w}}_i^{t+1}$ to the central server.

Updating $\gamma, \mathbf{w}_{\text{con}}$ in center server: After the central server receives all $\tilde{\mathbf{w}}_i^{t+1}$, it performs the following updates,

$$\mathbf{w}_{\text{con}}^{t+1} = \text{prox}_{\mu \|\cdot\|_1} \left(\frac{\sum_{i=1}^I \gamma_i \text{Proj}_{\mathcal{W}}(\tilde{\mathbf{w}}_i^{t+1})}{C_{\gamma}^t} \right). \quad (28)$$

The last step in central server is to update γ using the same way as (20). The main difference between this algorithm and Algorithm 1 is that we add Gaussian noise to the gradient in (26) to mask the contributions of each individual data point. However, we have no knowledge about how to determine the noise level so far. Adding too much noise will inevitably lead to a decrease in learning performance, but if the noise is too small, it will not meet the privacy requirements. In Section IV-D, we will provide a theoretical guidance to determine \mathbf{s}_i^t .

C. Convergence analysis

Before proceeding to the privacy analysis, we discuss the effect of adding noise on the algorithm convergence. To simplify the analysis, we assume the added noise in all iterations and clients is the same, i.e., $\sigma_i^t = \sigma$. The results can be easily extended to the case where σ_i^t varies.

Theorem 2. Suppose Assumptions 1-3 hold, and the added Gaussian noise is $\mathbf{s}_i^t \sim \text{Gauss}(0, \sigma)^p$, the sequences $\mathbf{w}_i^t, \mathbf{w}_{\text{con}}^t$ generated from our algorithm with DP satisfy

$$\frac{1}{T} \sum_{t=0}^{T-2} \left(\sum_{i=1}^I \mathbb{E} [\|\mathbf{w}_i^t - \mathbf{w}_i^{t-1}\|_2^2] \right) \leq \frac{C_1}{T} + \Delta_1 \quad (29)$$

$$\frac{1}{T} \sum_{t=0}^{T-1} \mathbb{E} [\|\mathbf{w}_{\text{con}}^t - \mathbf{w}_{\text{con}}^{t+1}\|_2^2] \leq \frac{C_2}{T} + \Delta_2, \quad (30)$$

where

$$\begin{aligned} C_1 &= \frac{2\Delta_3\eta_w}{1-\xi^2}, C_2 = \frac{2B_r\Delta_3}{\rho I}, \\ \Delta_1 &= \frac{2\sqrt{2p}\eta_w I \sigma (\xi B_r + \eta_w B_g) + 4pI\eta_w\sigma^2}{1-\xi^2}, \\ \Delta_2 &= \frac{2\sqrt{2p}IB_r\sigma (\xi B_r + \eta_w B_g) + 4pIB_r\sigma^2}{\rho I}, \\ \Delta_3 &= \sum_{i=1}^I \mathbb{E} [f_i(\mathbf{w}_i^0, \mathbf{w}_{\text{con}}^0)] - f_i^{\min} + \lambda\sqrt{p}B_r. \end{aligned} \quad (31)$$

Proof: See supplementary material for more details. ■

The results reveal that the average cumulative error of our algorithm consists of two terms. The first term is the same as that of Algorithm 1, which will decay to zero as the increase of T . The second term is incurred by the added noise, which will not decay as T . Therefore, the added noise causes a constant bias to the learned graph sequence. This bias undoubtedly is determined by the noise level σ .

D. Privacy analysis

In this subsection, we will illustrate how to scale \mathbf{s}_i^t to ensure that the randomized mechanism obtain the desired level of differential privacy, i.e., $(\bar{\epsilon}_i, \bar{\delta}_i)$.

Theorem 3. Suppose the randomized mechanism of i -th client is M_i . For some $\epsilon_i^t > 0, \delta_i^t \in [0, 1]$, let $\mathbf{s}_i^t \sim \text{Gauss}(0, \sigma_i^t)^p \in \mathbb{R}^p$, where $\sigma_i^t \geq \frac{2\sqrt{2\ln(1.25/\delta_i^t)}B_z}{N_i\epsilon_i^t}$. For any $\bar{\delta}_i$ and an initial point independent of \mathcal{D}_i , the mechanism $M_i(\mathcal{D}_i)$ is $(\bar{\epsilon}_i, 1 - (1 - \bar{\delta}_i) \prod_{t=1}^T (1 - \delta_i^t))$ -DP with

$$\begin{aligned} \bar{\epsilon}_i &= \min \left\{ \sum_{t=1}^T \epsilon_i^t, \sum_{t=1}^T \frac{(e^{\epsilon_i^t} - 1)\epsilon_i^t}{e^{\epsilon_i^t} + 1} \right. \\ & \quad \left. + \sqrt{\sum_{t=1}^T 2(\epsilon_i^t)^2 \log \left(e + \sqrt{\sum_{t=1}^T (\epsilon_i^t)^2 / \bar{\delta}_i} \right)} \right. \\ & \quad \left. + \sqrt{\sum_{t=1}^T \frac{(e^{\epsilon_i^t} - 1)\epsilon_i^t}{e^{\epsilon_i^t} + 1} + \sqrt{\sum_{t=1}^T 2(\epsilon_i^t)^2 \log(1/\bar{\delta}_i)}} \right\} \end{aligned} \quad (32)$$

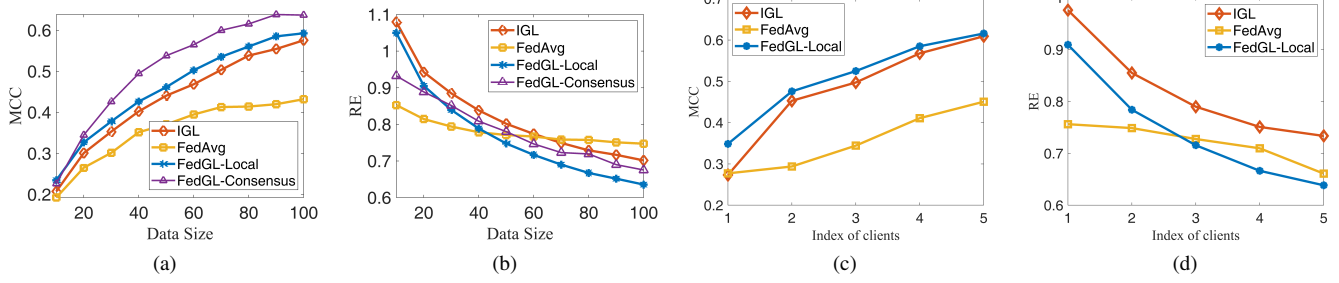


Fig. 2: The learned graphs of different data size. (a)-(b) The data size of all clients are set to be the same. (c)-(d) The data sizes of Clients 1-5 are set to be 20,40,60,80 and 100.

Proof: See Appendix C for more details. ■

The theorem theoretically determines the the minimum required noise level for a given $(\bar{\epsilon}_i, \bar{\delta}_i)$. It implies that when $\bar{\delta}_i = 0$, $M_i(\mathcal{D}_i)$ is $(\sum_{t=1}^T \epsilon_i^t, 0)$ - DP. We can obtain a better scaling for $\bar{\epsilon}_i$ at the cost of setting $\bar{\delta}_i > 0$ [45]. Furthermore, we find that the noise scale σ_i^t is inversely proportional to data size N_i of dataset \mathcal{D}_i , which is a classic property of DP. In practice, we may have no knowledge about the exact value of B_z and choose B_z as a large enough value. In this case, the obtained $\bar{\epsilon}$ might be too conservative, and the added noise is unnecessarily large. A practical trick is to clip the gradient to bound the influence of each individual example [46]. The most used clipping method is calculating the gradient of each sample in dataset. In this study, we clip the data vector $\tilde{\mathbf{z}}_{i,n} = \mathbf{z}_{i,n} / \max\left(1, \frac{\|\mathbf{z}_{i,n}\|_2}{C}\right)$, where C is a clipping threshold. The clipping ensures that if $\|\mathbf{z}_{i,n}\|_2 \geq C$, it gets scaled down to be of norm C . The final gradient is pair-wise distance vector is $\nabla g_i(\mathbf{w}) = \frac{1}{N_i} \sum_{n=1}^{N_i} \nabla g_i(\mathbf{w}, \tilde{\mathbf{z}}_{i,n})$. Using the clipping trick, we can replace B_z by C in Theorem 3. This can be easily checked using the proof in Appendix C.

V. EXPERIMENTS

In this section, we will test the performance of our proposed model using both synthetic data and real world data. Firstly, some experimental setups are introduced.

A. Experimental Setups

1) *Graph generation:* The top of the to-do list is generating real graphs for synthetic data. We generate a Gaussian radial basis function (RBF) random graph \mathcal{G}_0 with 20 vertices by following the method of [10]. The kernel function width is set to be 0.5. We then keep a certain proportion, e.g., q , of the existing edges in \mathcal{G}_0 unchanged, which form the consensus graph. We then add $(1-q)|\mathcal{E}_0|$ edges randomly to the common graph to form heterogeneous graphs $\mathcal{G}_1, \dots, \mathcal{G}_I$, where $|\mathcal{E}_0|$ is the number of edges of \mathcal{G}_0 . We use $1-q$ to represent graph and data heterogeneity in this study.

2) *Smooth graph signals generation:* For the graph of the i -th client, we first calculate the corresponding Laplacian matrix \mathbf{L}_i and then generate N_i graph signals from the Gaussian distribution defined by [10]

$$\mathbf{x}_{i,n} \sim \text{Gauss}\left(0, (\mathbf{L}_i + \sigma_w^2 \mathbf{I})^\dagger\right), \quad (33)$$

where σ_w^2 is the covariance of Gaussian noise, and we set $\sigma_w = 0.1$. As demonstrated in [11], graph signals generated in this way are smooth over the corresponding graphs.

3) *Evaluation metric:* In topology inference, determining whether two vertices are connected can be regarded as a binary classification problem. As a result, the first metric is Matthews correlation coefficient (MCC) [47], which is defined as

$$\text{MCC} = \frac{\text{TP} \cdot \text{TN} - \text{FP} \cdot \text{FN}}{\sqrt{(\text{TP} + \text{FP})(\text{TP} + \text{FN})(\text{TN} + \text{FP})(\text{TN} + \text{FN})}}, \quad (34)$$

where TP is true positive rate, TN is true negative rate, FP is false positive rate and FN denotes false negative rate. MCC is a comprehensive evaluation metric, and its value range is $[-1, +1]$. The value $+1$ means that we exactly learn the existence of all edges in the groundtruth, while -1 is interpreted as a total misidentification. The second metric is relative error (RE) for evaluating edge weights, i.e.,

$$\text{RE} = \frac{\|\mathbf{W}^* - \mathbf{W}_{\text{gt}}\|_F}{\|\mathbf{W}_{\text{gt}}\|_F}, \quad (35)$$

where \mathbf{W}^* is the learned adjacent matrix and \mathbf{W}_{gt} is the groundtruth. For consensus graph, we calculate RE and MCC between the learned \mathbf{w}_{con} and the real one. For local graphs, we calculate the average of the two metrics for all I graphs.

4) *Baselines:* Due to no existing models that focus on the problem of this study, we use the classic FL algorithm FedAvg [26] to solve the following problem as our baselines.

$$\min_{\mathbf{w} \in \mathcal{W}} \frac{1}{N} \sum_{i=1}^I \sum_{n=1}^{N_i} 2\mathbf{z}_{i,n}^\top \mathbf{w} - \alpha \mathbf{1}^\top \log(\mathbf{S}\mathbf{w}) + 2\beta \|\mathbf{w}\|_2^2, \quad (36)$$

where N is the number of all data. The problem learns a global graph \mathbf{w} using all data without considering data heterogeneity. We also adopt a baseline named IGL (independent graph learning), in which each client learns a graph independently using their local data. For our model, we use FedGL-Local to denote the average results of all local clients and FedGL-Common to represent the results of the consensus graph.

5) *Determination of parameters:* For our model, we fix α as 2 and search the best β for independent graph learning as our parameter. The value of ρ and λ are determined by grid search in different experimental cases. In our algorithm, we fix $C = 25$ for all synthetic data, which experimentally proves to be large enough that in practice almost no gradient needs to be clipped. The momentum weight ξ is set to be 0.9 and the stepsize η_w is 0.0005 that is small enough to satisfy

$\eta_w \leq 1/L_i$ for $i = 1, \dots, I$. Moreover, we set $K_i^t = 25$, $T = 8$ for all experiments. The number of clients for synthetic data are 5 in our experiment. All parameters of baselines are selected as those that achieve the best MCC value.

6) *Operating environment*: All algorithms are implemented by MATLAB and run on an Intel(R) CPU with 3.80GHz clock speed and 16GB of RAM.

B. Synthetic Data

1) *Data size*: We first check the impact of data size. We fix q as 0.5 and assume equal data size for all clients. The data size varies from 10 to 100, and the results are shown as Fig.2 (a)-(b). We find the graphs learned by FedAvg reaches the worst MCC since it learns a global graph using data from all clients. However, the graph heterogeneity is large in this experiment, meaning that the local graphs are quite different. Therefore, the learned global graph is far from local graphs. In sharp contrast, IGL learns graphs using local datasets independently and obtains increasing performance as data size. Our model also learns a personalized graph for each client. Different from IGL, we learn graphs of all clients jointly by “borrowing” information from each other via a consensus graph. Thus, our model has better performance than that of IGL for both MCC and RE. Moreover, from Fig.2 (a)-(b), the learned consensus graph also displays better performance than IGL and FedAvg. To check the impact of imbalance data sizes, we set N_i to be 20,40,60,80,100 for client 1-5 respectively. From Fig.2 (c)-(d), we find that clients with larger N_i can obtain better performance for all models. However, our model can improve the performance of clients with small data sizes because they can “borrow” information from clients with large data sizes.

2) *Data heterogeneity*: We next explore the impact of data heterogeneity. In this experiment, we fix $N_i = 50$ for all clients and vary q from 0.2 to 0.8. As displayed in Fig.3, we can find that when data heterogeneity is small, the FedAvg reaches the best performance since the global graph is close to the local graphs of each client. In this scenario, FedAvg benefits from using all data to learn a global graph. However, as the increase of q , the performance of FedAvg drastically decreases. On the contrary, our model suffers less from graph heterogeneity since we learn a personalized graph for each client. Furthermore, our model outperforms IGL because we learn all graphs jointly. Figure 4 provides the visualization of the learned graphs. We can observe that FedAvg performs the worst since the global graph can hardly learn the specific structures of the local graphs. Our model effectively captures the common and specific structures while IGL fails to find the common structures.

3) *Adaptive weights*: We also study the factors that affect the learned weights γ . Two factors are considered in this study, i.e., data size and data heterogeneity. For data size, we let q be 0.5 and set N_i as 20,40,60,80,100 for client 1-5, respectively. On the other hand, for data heterogeneity, we fix $N_i = 100$ and first generate a RBF random graph \mathcal{G}_1 for client 1. The graphs of client 2-4 are generated based on \mathcal{G}_1 with q equal to 0.2, 0.4, 0.6 and 0.8. The learned values of γ are displayed in Table I, and two trends can be observed. Firstly, graphs with large

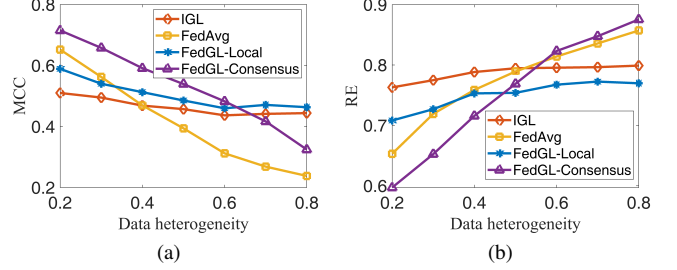


Fig. 3: The learned graphs of different data heterogeneity

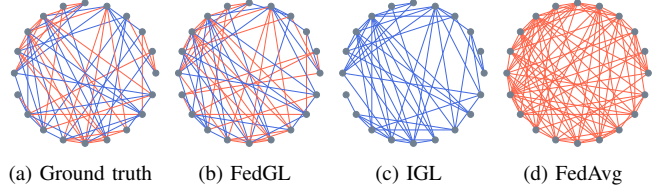


Fig. 4: The learned graphs of $q = 0.5$ and $N_i = 100$. In (a)-(b) The red edges are those in the consensus graphs. The blue edges represents the specific edges learned by local clients.

data sizes contribute more to the consensus graph. Secondly, those that are similar with \mathcal{G}_1 learn larger weights. Therefore, we can conclude that the adaptive weight adjustment strategy can effectively find those clients that contribute more to the consensus graph.

4) *Parameter sensitivity*: In this experiment, we set $q = 0.5$, $N_i = 100$ for all clients. Additionally, we also let $\alpha = 2$ and $\beta = 1.5$ to check the impact of different choices of λ and ρ . For λ , we fix $\rho = 0.3$ and vary λ from 0.01 to 1. As shown in Fig.5(a), the performance of local graphs is hardly affected by the choice of λ . However, the learned consensus graphs rely heavily on the choice of λ , since λ controls the sparsity of consensus graphs. There exists an optimal λ that make consensus graph reach the best performance for both MCC and RE. On the other hand, we fix $\lambda = 0.2$ and vary ρ from 0.1 to 50 to check the impact of ρ . Similarly, the consensus graphs are more sensitive to ρ . In this experiment, we find that local graphs also depend on the choice of ρ . Basically, the best ρ is the same as that of consensus graphs.

5) *Differential privacy*: In this experiment, we fix $q = 0.5$, $\bar{\epsilon}_i = \bar{\epsilon}$ and $\bar{\delta} = 10^{-5}$. We simply split privacy budget $\bar{\epsilon}$ across all iterations $T = 8$. The Gaussian noise is added to each client by following the Theorem 3. Firstly, we vary N_i from 50 to 1000 and check the performance, i.e., RE, of the learned local graphs. As depicted in Fig.6 (a), our model without DP reaches the best performance. When we consider differential privacy, the performance will decrease since we add noise to the gradients. Smaller $\bar{\epsilon}$ means stronger privacy protection, and hence more noise is added, resulting worse performance. In general, our algorithms with DP outperform IGL, a perfectly private baseline, and further guarantee a certain level of privacy protection. For small $\bar{\epsilon}$, e.g., $\bar{\epsilon} = 0.3$, our algorithm fails to obtain better performance than IGL since the added noise affects the performance. However, it can regain its advantage when data size is large. Therefore,

TABLE I: The learned γ in different scenarios

Client Index	1	2	3	4	5
Data size	0.541	0.584	0.661	0.707	0.718
Graph heterogeneity	0.837	0.808	0.720	0.735	0.584

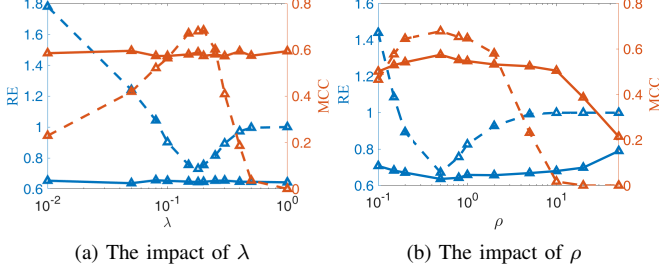


Fig. 5: The impact of parameter selections. The blue and red lines represent the results of RE and MCC respectively. The solid and dashed lines represent the results of local graphs and consensus graphs respectively.

the choice of $\bar{\epsilon}$ is a trade-off between privacy consideration and learning performance. Fig.6 (b) shows the convergence of our algorithms. In this experiment, we fix $N_i = 100$ for $i = 1, \dots, 5$. As stated in Theorem 1 and 2, the Fig.6 (b) proves that both algorithms with and without DP can reach convergence in a few interactions. The number needed for convergence can be adjusted by setting different K_i^t . Usually, to reduce communication cost and preserve privacy, we hope T to be a small number. However, large K_i^t indicates that the central server needs more waiting time to receive updated models from all local clients. Thus, the choice of K_i^t depends on application requirements. The results also imply that we can further improve the performance of the algorithms with DP by reducing T , since $T = 8$ is larger than the required iterations for convergence.

C. Real-world Data

1) *Social network*: We first consider social networks from the Ljubljana student network dataset¹. The dataset contains 12 network whose nodes represents the same 32 students. The edges captures interactions among these students. The interactions are built based on the students' answers to different questions that might be related to private privacy. A total of 12 questions are asked, corresponding to 12 graphs. We suppose the questions are asked by different organizations. We select three networks and regard the corresponding organizations as local clients. Since these organizations do not wish to share private data, we need to learn the graphs under privacy constraints. Furthermore, graphs related to different questions should share some common structures (friends of these students) due to that all answers come from the same students. Note that the dataset does not contain graph signals, and we generate signals for each network using (33). The data sizes of each client are the same and are ranging from 100 to 400. The results displayed in Fig.7 illustrate that our

¹The data is available at <http://vladowiki.fmf.uni-lj.si/doku.php?id=pajek:dataset:pajek:students>

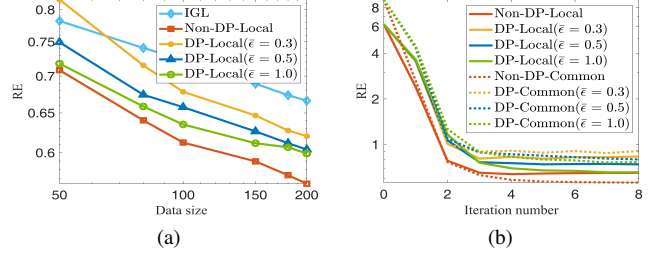


Fig. 6: The learned graphs of DP. (a) The results of different data sizes. (b) The results of convergence.

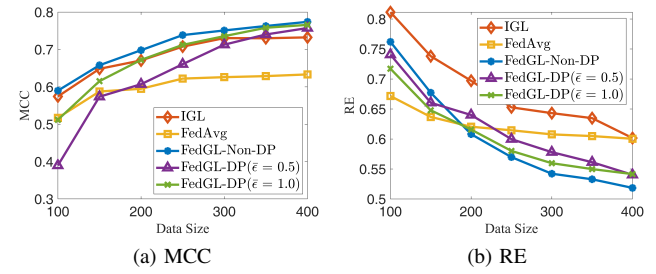


Fig. 7: The results of the learned graphs of social network

model without DP reaches the best performance as expected. Additionally, the algorithms with DP outperform IGL and at the same time preserve data privacy.

2) *COIL-20 data*: We next employ the COIL20 data² to learn the relationships between images. The COIL-20 dataset is a collection of gray-scale images, including 20 objects taken from different angles (taking a picture every 5 degrees). The size of each image is 32×32 , and each object has 72 images. We select 4 objects, and for each object, images of three different views, i.e., views from the taken degree $[0^\circ, 55^\circ]$, $[60^\circ, 115^\circ]$ and $[120^\circ, 175^\circ]$, are thought to be taken from three photographers. Each photographer have 48 images, 12 of each object. We take each image as a node, and aim to learn the relationships between these images. The image itself is taken as graph signals, i.e., $\mathbf{X}_i \in \mathbb{R}^{48 \times 1024}$. We suppose that the photographers are not willing to share their photos, and hence all graphs are learned jointly under privacy constraints. Moreover, it is reasonable to assume that the graphs of images taken by three different photographers share common structures owing to that they come from the same objects. In addition, the learned graphs should have 4 clusters since the 48 images belong to four objects. To evaluate the learned graphs, we adopt the classic Louvain method [48] to detect the communities in the learned graphs. Three commonly used metrics, i.e., normalized mutual information (NMI), Fowlkes and Mallows index (FMI) [49] and Rand Index (RI) are adopted to evaluate the detection results. The labels of the images are taken as the groundtruth. For our model, we use the learned consensus graph to find communities, since the consensus graph captures the common structure of all local graphs, which may remove noisy edges of different views. The

²The data are available at <https://www.cs.columbia.edu/CAVE/software/softlib/coil-20.php>

TABLE II: The detection results of different models. For IGL, we list the results of all three local clients, i.e., \mathcal{C}_1 - \mathcal{C}_3 .

	IGL \mathcal{C}_1	IGL \mathcal{C}_2	IGL \mathcal{C}_3	FedAvg	FedGL Non-DP	FedGL $\bar{\epsilon} = 0.5$	FedGL $\bar{\epsilon} = 1.0$
NMI	0.857	0.839	0.857	0.857	1	1	1
RI	0.872	0.894	0.872	0.872	1	1	1
FMI	0.804	0.796	0.804	0.804	1	1	1

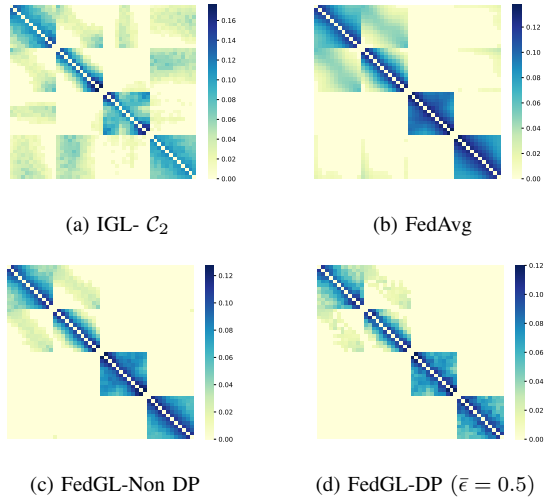


Fig. 8: Some visualizations of the learned graphs

detection results are listed in Table II. Our model succeeds to find all communities in the graphs, even for the algorithms with DP, while both IGL and FedAvg make mistakes more or less. As shown in Fig.8, the communities can be clearly observed in the graphs learned by our models. However, more confusing edges appear in the graphs of IGL and FedAvg.

3) *Medical data*: We employ fMRI data to learn brain functional connectivity graphs to advance autism study. The basic assumption is that the autism may affect brain functional connectivity. Consequently, if we can learn about the differences in brain functional connectivity graphs between autistic suffers and normal people, it may help us better understand the mechanism of autism. However, medical data are privacy-sensitive, and their transmission to an unreliable central servers is usually prohibited. Hence, our proposed algorithm is perfect for this situation. The data we employ is blood-oxygenation-level-dependent (BOLD) time series extracted from fMRI data. The used dataset³ contains 539 autistic patients and 573 typical controls. We select an autistic subject and a control to learn a graph of brain functional region connectivity for each subject. We select 34 functional regions of interest from 90 standard regions of Anatomical Automatic Labeling (AAL) template. As depicted in Fig.9, the graphs of autistic patients and normal people share many common edges. However, from the graphs learned by our models, we can observe some noticeable topological changes due to the affect of autism, which may aid in the diagnosis of autism. On the other hand, the differences between the graphs learned

by IGL are not as pronounced as ours. Furthermore, our model provides a consensus graph that captures the underlying common structures. The remaining heterogeneous parts may reflect information useful for autism diagnosis. We can also find that the method with DP can still learn the graphs that captures the different connections between normal and autistic people. Unfortunately, our knowledge does not allow us to interpret these results from a medical perspective. In the future, a domain expert might be helpful.

VI. CONCLUSION

In this paper, we are committed to the problem of learning graphs under privacy concerns using data located in distributed clients. We propose a framework to learn a consensus graph and a personalized graph for each client. An algorithm based on federated learning framework is proposed, in which all private data in processed in local clients. To further enhance privacy, we leverage differential privacy to prevent information of raw data from being leaking from transmitting model updates. A theoretical analysis is provided to guide how to ensure that our algorithm satisfies differential privacy. Extensive experiments are carried out and show that our algorithm can effectively learn meaningful graphs in the scenario. Future research directions include generalizing our framework to directed pattern structures as well as other graph learning methods except smoothness assumption.

APPENDIX A PROOF OF PROPOSITION 1

The proof is mainly derived from [50] but with some modifications. For two vectors \mathbf{a} and \mathbf{b} in $\tilde{\mathcal{W}}$, we have that

$$\begin{aligned}
 & \|\nabla_{\mathbf{a}} f_i(\mathbf{a}, \mathbf{w}_{\text{con}}) - \nabla_{\mathbf{b}} f_i(\mathbf{b}, \mathbf{w}_{\text{con}})\|_2 \\
 &= \left\| 4\beta(\mathbf{a} - \mathbf{b}) - \alpha \mathbf{S}^T \left(\frac{1}{\mathbf{S}\mathbf{a}} - \frac{1}{\mathbf{S}\mathbf{b}} \right) + \rho \gamma_i (\mathbf{a} - \mathbf{b}) \right\|_2 \\
 &\leq 4\beta \|\mathbf{a} - \mathbf{b}\|_2 + \alpha \|\mathbf{S}^T\|_2 \left\| \frac{1}{\mathbf{S}\mathbf{a}} - \frac{1}{\mathbf{S}\mathbf{b}} \right\|_2 + \rho \gamma_i \|\mathbf{a} - \mathbf{b}\|_2 \\
 &\leq 4\beta \|\mathbf{a} - \mathbf{b}\|_2 + \frac{\alpha \|\mathbf{S}\|_2}{\min(\mathbf{S}\mathbf{a}) \min(\mathbf{S}\mathbf{b})} \|\mathbf{S}\mathbf{a} - \mathbf{S}\mathbf{b}\|_2 + \rho \gamma_i \|\mathbf{a} - \mathbf{b}\|_2 \\
 &\leq 4\beta \|\mathbf{a} - \mathbf{b}\|_2 + \frac{\alpha \|\mathbf{S}\|_2^2}{\deg_{\min}^2} \|\mathbf{a} - \mathbf{b}\|_2 + \rho \gamma_i \|\mathbf{a} - \mathbf{b}\|_2 \\
 &= \left(4\beta + \frac{2\alpha(d-1)}{\deg_{\min}^2} + \rho \gamma_i \right) \|\mathbf{a} - \mathbf{b}\|_2 \triangleq L_i \|\mathbf{a} - \mathbf{b}\|_2, \quad (37)
 \end{aligned}$$

Since the stepsize η_w is supposed to be smaller than L_i in Assumption 3, we claim that \deg_{\min} exists and is greater than 0. The first inequality holds due to triangle inequality, while the last equality holds due to Assumption 1-2 and Lemma 1 in [50]. From (37), we can conclude that f_i is L_i -Lipschitz smooth w.r.t. \mathbf{w}_i on $\tilde{\mathcal{W}}$. On the other hand, we obtain that

$$\|\nabla_{\mathbf{a}} f(\mathbf{w}_i, \mathbf{a}) - \nabla_{\mathbf{b}} f(\mathbf{w}_i, \mathbf{b})\|_2 = \rho \gamma_i \|\mathbf{a} - \mathbf{b}\|_2 \quad (38)$$

Therefore, f_i is $\rho \gamma_i$ -Lipschitz smooth w.r.t. \mathbf{w}_{con} . The last part of the proof is to calculate the bound of the gradient of f_i w.r.t. \mathbf{w}_i . Specifically, for any $\mathbf{a} \in \tilde{\mathcal{W}}$, we have

$$\begin{aligned}
 & \|\nabla_{\mathbf{a}} f(\mathbf{a}, \mathbf{w}_{\text{con}})\|_2 \\
 &= \left\| \frac{1}{N_i} \sum_n^{N_i} 2\mathbf{z}_n + 4\beta\mathbf{a} - \alpha \mathbf{S}^T \left(\frac{1}{\mathbf{S}\mathbf{a}} \right) + \rho \gamma_i (\mathbf{a} - \mathbf{w}_{\text{con}}) \right\|_2
 \end{aligned}$$

³<http://preprocessed-connectomes-project.org/abide/>

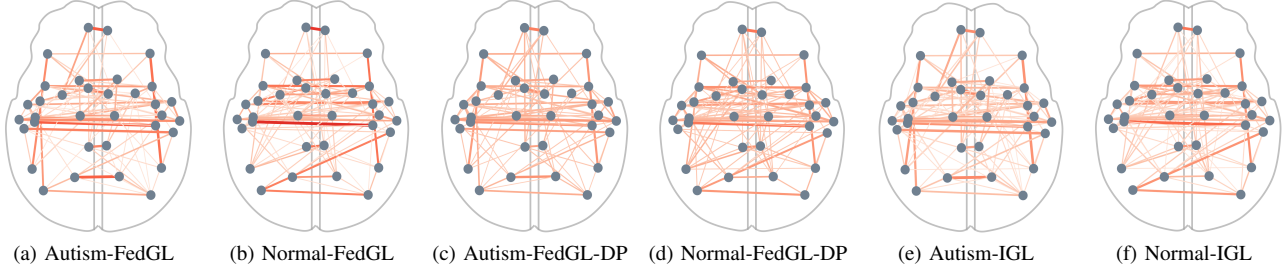


Fig. 9: The learned graphs of brain functional connectivity. The level of DP is ($\bar{\epsilon} = 0.5, \bar{\sigma} = 10^{-5}$)

$$\begin{aligned} &\leq \frac{2}{N_i} \sum_n^{N_i} \|\mathbf{z}_{i,n}\|_2 + 4\beta \|\mathbf{a}\|_2 + \alpha \|\mathbf{S}\|_2 \left\| \frac{1}{\mathbf{S}\mathbf{a}} \right\|_2 \\ &\quad + \rho\gamma_i \|\mathbf{a} - \mathbf{w}_{\text{con}}\|_2 \\ &\leq 2B_z + (4\beta + \rho\gamma_i)B_w + \alpha \frac{\sqrt{2d(d-1)}}{\deg_{\min}} \triangleq B_g, \end{aligned} \quad (39)$$

where the first inequality holds due to triangle inequality, and the second inequality holds due to Assumption 1-2 and Lemma 1 in [50].

APPENDIX B PROOF OF THEOREM 1

Before we start the proof, some lemmas are provided.

Lemma 1. Suppose that Assumption 1-3 hold, for any client i , the updated \mathbf{w}_i^{t+1} satisfies that

$$\begin{aligned} f_i(\mathbf{w}_i^{t+1}, \mathbf{w}_{\text{con}}^t) &\leq f_i(\mathbf{w}_i^t, \mathbf{w}_{\text{con}}^t) - \frac{1}{2\eta_w} \|\mathbf{w}_i^{t+1} - \mathbf{w}_i^t\|_2^2 \\ &\quad + \frac{\xi^2}{2\eta_w} \|\mathbf{w}_i^t - \mathbf{w}_i^{t-1}\|_2^2 \end{aligned} \quad (40)$$

Proof: Recall that f_i is convex and L_i -Lipschitz smooth w.r.t. \mathbf{w}_i as Proposition 1 states, we obtain that

$$\begin{aligned} f_i(\mathbf{w}_i^{t+1}, \mathbf{w}_{\text{con}}^t) &\leq f_i(\mathbf{w}_{i,\text{ex}}^t, \mathbf{w}_{\text{con}}^t) + \frac{L_i}{2} \|\mathbf{w}_i^{t+1} - \mathbf{w}_{i,\text{ex}}^t\|_2^2 \\ &\quad + \langle \nabla_{\mathbf{w}_i} f_i(\mathbf{w}_{i,\text{ex}}^t, \mathbf{w}_{\text{con}}^t), \mathbf{w}_i^{t+1} - \mathbf{w}_{i,\text{ex}}^t \rangle \end{aligned} \quad (41)$$

$$\begin{aligned} f_i(\mathbf{w}_i^t, \mathbf{w}_{\text{con}}^t) &\geq f_i(\mathbf{w}_{i,\text{ex}}^t, \mathbf{w}_{\text{con}}^t) \\ &\quad + \langle \nabla_{\mathbf{w}_i} f_i(\mathbf{w}_{i,\text{ex}}^t, \mathbf{w}_{\text{con}}^t), \mathbf{w}_i^t - \mathbf{w}_{i,\text{ex}}^t \rangle, \end{aligned} \quad (42)$$

where the first inequality holds because of the definition of L_i -Lipschitz smooth and the second inequality holds since f_i is a convex function. Combining the two inequalities, we have

$$\begin{aligned} &f_i(\mathbf{w}_i^{t+1}, \mathbf{w}_{\text{con}}^t) \\ &\leq f_i(\mathbf{w}_i^t, \mathbf{w}_{\text{con}}^t) + \langle \nabla_{\mathbf{w}_i} f_i(\mathbf{w}_{i,\text{ex}}^t, \mathbf{w}_{\text{con}}^t), \mathbf{w}_i^{t+1} - \mathbf{w}_i^t \rangle \\ &\quad + \frac{1}{2\eta_w} \|\mathbf{w}_i^{t+1} - \mathbf{w}_{i,\text{ex}}^t\|_2^2 \\ &\leq f_i(\mathbf{w}_i^t, \mathbf{w}_{\text{con}}^t) + \left\langle \frac{1}{\eta_w} (\mathbf{w}_i^{t+1} - \mathbf{w}_{i,\text{ex}}^t), \mathbf{w}_i^t - \mathbf{w}_i^{t+1} \right\rangle \\ &\quad + \frac{1}{2\eta_w} \|\mathbf{w}_i^{t+1} - \mathbf{w}_{i,\text{ex}}^t\|_2^2 \\ &\leq f_i(\mathbf{w}_i^t, \mathbf{w}_{\text{con}}^t) - \frac{1}{2\eta_w} \|\mathbf{w}_i^{t+1} - \mathbf{w}_i^t\|_2^2 + \frac{1}{2\eta_w} \|\mathbf{w}_i^t - \mathbf{w}_{i,\text{ex}}^t\|_2^2 \\ &\leq f_i(\mathbf{w}_i^t, \mathbf{w}_{\text{con}}^t) - \frac{1}{2\eta_w} \|\mathbf{w}_i^{t+1} - \mathbf{w}_i^t\|_2^2 + \frac{\xi^2}{2\eta_w} \|\mathbf{w}_i^t - \mathbf{w}_i^{t-1}\|_2^2 \end{aligned} \quad (43)$$

where the second inequality holds due to (15) and the following first-order optimality condition that holds for any $\tilde{\mathbf{w}}_i \in \mathcal{W}$.

$$\left\langle \nabla_{\mathbf{w}_i} f_i(\mathbf{w}_{i,\text{ex}}^t, \mathbf{w}_{\text{con}}^t) + \frac{1}{\eta_w} (\mathbf{w}_i^{t+1} - \mathbf{w}_{i,\text{ex}}^t), \tilde{\mathbf{w}}_i - \mathbf{w}_i^{t+1} \right\rangle \geq 0. \quad (44)$$

The third inequality holds since

$$\begin{aligned} &\langle \mathbf{w}_i^{t+1} - \mathbf{w}_{i,\text{ex}}^t, \mathbf{w}_i^t - \mathbf{w}_i^{t+1} \rangle \\ &= \frac{1}{2} (\|\mathbf{w}_i^t - \mathbf{w}_{i,\text{ex}}^t\|_2^2 - \|\mathbf{w}_i^{t+1} - \mathbf{w}_{i,\text{ex}}^t\|_2^2 - \|\mathbf{w}_i^{t+1} - \mathbf{w}_i^t\|_2^2). \end{aligned} \quad (45)$$

Finally, we complete the proof. \blacksquare

Lemma 2. Suppose Assumption 2-3 hold, the updated $\mathbf{w}_{\text{con}}^{t+1}$ satisfies that

$$\begin{aligned} &\sum_i^I f_i(\mathbf{w}_i^{t+1}, \mathbf{w}_{\text{con}}^{t+1}) + \lambda \|\mathbf{w}_{\text{con}}^{t+1}\|_1 \\ &\leq \sum_i^I f_i(\mathbf{w}_i^{t+1}, \mathbf{w}_{\text{con}}^t) + \lambda \|\mathbf{w}_{\text{con}}^t\|_1 - \frac{\rho C_\gamma^t}{2} \|\mathbf{w}_{\text{con}}^{t+1} - \mathbf{w}_{\text{con}}^t\|_2^2. \end{aligned} \quad (46)$$

Proof: For simplicity, we first define $F(\mathbf{w}_{\text{con}}) = \sum_i^I f_i(\mathbf{w}_i^{t+1}, \mathbf{w}_{\text{con}})$. Since $f_i(\mathbf{w}_i^{t+1}, \mathbf{w}_{\text{con}})$ is $\rho\gamma_i^t$ -convex w.r.t. \mathbf{w}_{con} , $F(\mathbf{w}_{\text{con}})$ is ρC_γ^t -convex w.r.t. \mathbf{w}_{con} , and we obtain

$$\begin{aligned} F(\mathbf{w}_{\text{con}}^{t+1}) &\leq F(\mathbf{w}_{\text{con}}^t) + \langle \nabla F(\mathbf{w}_{\text{con}}^t), \mathbf{w}_{\text{con}}^{t+1} - \mathbf{w}_{\text{con}}^t \rangle \\ &\quad + \frac{\rho C_\gamma^t}{2} \|\mathbf{w}_{\text{con}}^{t+1} - \mathbf{w}_{\text{con}}^t\|_2^2. \end{aligned} \quad (47)$$

On the other hand, due to the convexity of $F(\mathbf{w}_{\text{con}}^{t+1})$, for any $\mathbf{y} \in \mathcal{W}$, we have $F(\mathbf{y}) \geq F(\mathbf{w}_{\text{con}}^t) + \langle \nabla F(\mathbf{w}_{\text{con}}^t), \mathbf{y} - \mathbf{w}_{\text{con}}^t \rangle$. Combining it with (47), we finally reach that

$$\begin{aligned} F(\mathbf{w}_{\text{con}}^{t+1}) &\leq F(\mathbf{y}) - \langle \nabla F(\mathbf{w}_{\text{con}}^t), \mathbf{y} - \mathbf{w}_{\text{con}}^t \rangle \\ &\quad + \langle \nabla F(\mathbf{w}_{\text{con}}^t), \mathbf{w}_{\text{con}}^{t+1} - \mathbf{w}_{\text{con}}^t \rangle + \frac{\rho C_\gamma^t}{2} \|\mathbf{w}_{\text{con}}^{t+1} - \mathbf{w}_{\text{con}}^t\|_2^2. \end{aligned} \quad (48)$$

We next focus on $h(\mathbf{w}_{\text{con}}) = \|\mathbf{w}_{\text{con}}\|_1$. Recall that $\mathbf{w}_{\text{con}}^{t+1} = \text{prox}_{\mu \|\cdot\|_1} \left(\frac{\sum_{i=1}^I \gamma_i \mathbf{w}_i^{t+1}}{C_\gamma^t} \right) = \arg\min \frac{1}{2} \left\| \mathbf{w}_{\text{con}} - \frac{\sum_{i=1}^I \gamma_i \mathbf{w}_i^{t+1}}{C_\gamma^t} \right\|_2^2 + \frac{\lambda}{\rho} \|\mathbf{w}_{\text{con}}\|_1$. Define $\frac{\sum_{i=1}^I \gamma_i \mathbf{w}_i^{t+1}}{C_\gamma^t} = \mathbf{w}_{\text{avg}}^{t+1}$, by optimal conditions we obtain

$$\begin{aligned} 0 &\in \frac{\rho}{\lambda} (\mathbf{w}_{\text{con}}^{t+1} - \mathbf{w}_{\text{avg}}^{t+1}) + \partial h(\mathbf{w}_{\text{con}}^{t+1}) \\ &\implies \frac{\rho}{\lambda} (\mathbf{w}_{\text{avg}}^{t+1} - \mathbf{w}_{\text{con}}^{t+1}) \in \partial h(\mathbf{w}_{\text{con}}^{t+1}) \end{aligned} \quad (49)$$

Similarly, due to the convexity of $h(\mathbf{w}_{\text{con}})$, we have $h(\mathbf{y}) \geq h(\mathbf{w}_{\text{con}}^{t+1}) + \langle \partial h(\mathbf{w}_{\text{con}}^{t+1}), \mathbf{y} - \mathbf{w}_{\text{con}}^{t+1} \rangle$. Combining it with (48) and (49), we obtain

$$\begin{aligned} F(\mathbf{w}_{\text{con}}^{t+1}) + \lambda h(\mathbf{w}_{\text{con}}^{t+1}) &\leq F(\mathbf{y}) + \lambda h(\mathbf{y}) + \langle \nabla F(\mathbf{w}_{\text{con}}^t) \\ &\quad + \rho (\mathbf{w}_{\text{avg}}^{t+1} - \mathbf{w}_{\text{con}}^{t+1}), \mathbf{w}_{\text{con}}^{t+1} - \mathbf{y} \rangle + \frac{\rho C_\gamma^t}{2} \|\mathbf{w}_{\text{con}}^{t+1} - \mathbf{w}_{\text{con}}^t\|_2^2 \\ &\implies F(\mathbf{w}_{\text{con}}^{t+1}) + \lambda h(\mathbf{w}_{\text{con}}^{t+1}) \leq F(\mathbf{y}) + \lambda h(\mathbf{y}) \\ &\quad + \langle \mathbf{w}_{\text{con}}^t - \mathbf{w}_{\text{con}}^{t+1}, \mathbf{w}_{\text{con}}^{t+1} - \mathbf{y} \rangle + \frac{\rho C_\gamma^t}{2} \|\mathbf{w}_{\text{con}}^{t+1} - \mathbf{w}_{\text{con}}^t\|_2^2 \\ &\stackrel{\mathbf{y} = \mathbf{w}_{\text{con}}^t}{\implies} F(\mathbf{w}_{\text{con}}^{t+1}) + \lambda h(\mathbf{w}_{\text{con}}^{t+1}) \leq F(\mathbf{w}_{\text{con}}^t) + \lambda h(\mathbf{w}_{\text{con}}^t) \\ &\quad - \frac{\rho C_\gamma^t}{2} \|\mathbf{w}_{\text{con}}^{t+1} - \mathbf{w}_{\text{con}}^t\|_2^2 \end{aligned} \quad (50)$$

Finally, we complete the proof. \blacksquare

Equipped with the two lemmas, we start our proof of Theorem 1. For rotational simplicity, we fix $K_i^t = 1$ and omit the inner iteration index k . The following proof can be easily extended to the case where $K_i^t > 1$. We next define some symbols to simplify the expression. Specifically,

$$\begin{aligned} E_{\mathbf{w}_i}^t &= \sum_{i=1}^I f_i(\mathbf{w}_i^t, \mathbf{w}_{\text{con}}^t) - f_i(\mathbf{w}_i^{t+1}, \mathbf{w}_{\text{con}}^t) \\ E_{\mathbf{w}_{\text{con}}}^t &= \sum_{i=1}^I f_i(\mathbf{w}_i^{t+1}, \mathbf{w}_{\text{con}}^t) + \lambda \|\mathbf{w}_{\text{con}}^t\|_1 - f_i(\mathbf{w}_i^{t+1}, \mathbf{w}_{\text{con}}^{t+1}) \\ &\quad + \lambda \|\mathbf{w}_{\text{con}}^{t+1}\|_1 \\ e_{\mathbf{w}_i}^t &= \frac{1}{2\eta_w} \mathbb{E}[\|\mathbf{w}_i^{t+1} - \mathbf{w}_i^t\|_2^2] - \frac{\xi^2}{2\eta_w} \mathbb{E}[\|\mathbf{w}_i^t - \mathbf{w}_i^{t-1}\|_2^2] \\ e_{\mathbf{w}_{\text{con}}}^t &= \frac{\rho C_\gamma^t}{2} \|\mathbf{w}_{\text{con}}^t - \mathbf{w}_{\text{con}}^{t+1}\|_2^2 \end{aligned} \quad (51)$$

Then combining Lemma 1 and Lemma 2, we have

$$\sum_{i=1}^I e_{\mathbf{w}_i}^t + e_{\mathbf{w}_{\text{con}}}^t \leq E_{\mathbf{w}_i}^t + E_{\mathbf{w}_{\text{con}}}^t. \quad (52)$$

Summing (52) from 0 to $T-1$, we obtain

$$\begin{aligned} &\sum_{t=0}^{T-1} \sum_{i=1}^I e_{\mathbf{w}_i}^t + e_{\mathbf{w}_{\text{con}}}^t \leq \sum_{t=0}^{T-1} E_{\mathbf{w}_i}^t + E_{\mathbf{w}_{\text{con}}}^t \\ &= \sum_{i=1}^I f_i(\mathbf{w}_i^0, \mathbf{w}_{\text{con}}^0) - f_i(\mathbf{w}_i^T, \mathbf{w}_{\text{con}}^T) + \lambda \|\mathbf{w}_{\text{con}}^0\|_1 - \lambda \|\mathbf{w}_{\text{con}}^T\|_1 \\ &\leq \sum_{i=1}^I f_i(\mathbf{w}_i^0, \mathbf{w}_{\text{con}}^0) - f_i^{\min} + \lambda \|\mathbf{w}_{\text{con}}^0 - \mathbf{w}_{\text{con}}^T\|_1 \\ &\leq \sum_{i=1}^I f_i(\mathbf{w}_i^0, \mathbf{w}_{\text{con}}^0) - f_i^{\min} + \lambda \sqrt{p} \|\mathbf{w}_{\text{con}}^0 - \mathbf{w}_{\text{con}}^T\|_2 \\ &\leq \sum_{i=1}^I f_i(\mathbf{w}_i^0, \mathbf{w}_{\text{con}}^0) - f_i^{\min} + \lambda \sqrt{p} B_r \triangleq \Delta, \end{aligned} \quad (53)$$

where f_i^{\min} denotes the minimum of f_i . Notice that

$$\begin{aligned} \sum_{t=0}^{T-1} e_{\mathbf{w}_i}^t &= \sum_{t=0}^{T-1} \left(\frac{1}{2\eta_w} \|\mathbf{w}_i^{t+1} - \mathbf{w}_i^t\|_2^2 - \frac{\xi^2}{2\eta_w} \|\mathbf{w}_i^t - \mathbf{w}_i^{t-1}\|_2^2 \right) \\ &\geq \sum_{t=0}^{T-2} \frac{1 - \xi^2}{2\eta_w} \|\mathbf{w}_i^{t+1} - \mathbf{w}_i^t\|_2^2 - \frac{1}{2\eta_w} \|\mathbf{w}_i^0 - \mathbf{w}_i^{-1}\|_2^2 \\ &= \sum_{t=0}^{T-2} \frac{1 - \xi^2}{2\eta_w} \|\mathbf{w}_i^{t+1} - \mathbf{w}_i^t\|_2^2. \end{aligned} \quad (54)$$

We expand the summation operator to obtain the first inequality. The last equality holds due to initialization conditions of our algorithm. With (53) and (54), we obtain that

$$\frac{1}{T} \sum_{t=0}^{T-2} \sum_{i=1}^I \frac{1 - \xi^2}{2\eta_w} \|\mathbf{w}_i^{t+1} - \mathbf{w}_i^t\|_2^2 + \frac{1}{T} \sum_{t=0}^{T-1} e_{\mathbf{w}_{\text{con}}}^t \leq \frac{\Delta}{T}, \quad (55)$$

Since $0 \leq \xi < 1$, we can conclude that

$$\frac{1}{T} \sum_{t=0}^{T-2} \left(\sum_{i=1}^I \mathbb{E}[\|\mathbf{w}_i^{t+1} - \mathbf{w}_i^t\|_2^2] \right) = \frac{C_1}{T}, \quad (56)$$

where $C_1 = \frac{2\Delta\eta_w}{(1-\xi^2)}$.

In the same way, we obtain that

$$\begin{aligned} \frac{1}{T} \sum_{t=0}^{T-1} e_{\mathbf{w}_{\text{con}}}^t &\leq \frac{\Delta}{T} \\ \implies \frac{\rho}{2T} \sum_{t=0}^{T-1} C_\gamma^t \|\mathbf{w}_{\text{con}}^t - \mathbf{w}_{\text{con}}^{t+1}\|_2^2 &\leq \frac{\Delta}{T} \\ \implies \frac{\rho I}{2TB_r} \sum_{t=0}^{T-1} \|\mathbf{w}_{\text{con}}^t - \mathbf{w}_{\text{con}}^{t+1}\|_2^2 &\leq \frac{\Delta}{T} \\ \implies \frac{1}{T} \sum_{t=0}^{T-1} \mathbb{E}[\|\mathbf{w}_{\text{con}}^t - \mathbf{w}_{\text{con}}^{t+1}\|_2^2] &\leq \frac{C_2}{T} \end{aligned} \quad (57)$$

where $C_2 = \frac{2B_r\Delta}{\rho I}$. The third inequality holds since $C_\gamma^t = \sum_{i=1}^I \gamma_i^t = \sum_{i=1}^I 1/\|\mathbf{w}_i^{t-1} - \mathbf{w}_{\text{con}}^{t-1}\|_2 \geq \sum_{i=1}^I 1/Br = I/Br$.

APPENDIX C PROOF OF THEOREM 3

Firstly, we care about the sensitivity of the update of $\check{\mathbf{w}}_i^{t+1}$. For two neighbouring datasets $\mathcal{D}_i^1 = \{\mathbf{z}_{i,1}, \dots, \mathbf{z}_{i,n}^1, \dots, \mathbf{z}_{i,N_i}\}$ and $\mathcal{D}_i^2 = \{\mathbf{z}_{i,1}, \dots, \mathbf{z}_{i,n}^2, \dots, \mathbf{z}_{i,N_i}\}$, where $\mathbf{z}_{i,n}^1$ and $\mathbf{z}_{i,n}^2$ are the only difference between the two datasets.

$$\begin{aligned} &\text{sensitivity}(\check{\mathbf{w}}_i^{t+1}) \\ &= \max_{\mathcal{D}_i^1, \mathcal{D}_i^2} \left\| (\check{\mathbf{w}}_i^{t+1})_{\mathcal{D}_i^1} - (\check{\mathbf{w}}_i^{t+1})_{\mathcal{D}_i^2} \right\|_2 \\ &= \max_{\mathcal{D}_i^1, \mathcal{D}_i^2} \eta_w \left\| \nabla g_i \left(\mathbf{w}_{i,\text{ex}}^{t,K_i^t-1}; \mathcal{D}^2 \right) - \nabla g_i \left(\mathbf{w}_{i,\text{ex}}^{t,K_i^t-1}; \mathcal{D}^1 \right) \right\|_2 \\ &= \max \frac{2\eta_w}{N_i} \left\| \sum_{\mathbf{z}^2 \in \mathcal{D}^2} \mathbf{z}^2 - \sum_{\mathbf{z}^1 \in \mathcal{D}^1} \mathbf{z}^1 \right\|_2 \\ &= \frac{2\eta_w}{N_i} \max \|\mathbf{z}_{i,n}^1 - \mathbf{z}_{i,n}^2\|_2 \leq \frac{2\eta_w}{N_i} \max \|\mathbf{z}_{i,n}\|_2 \triangleq \frac{2\eta_w B_z}{N_i}, \end{aligned} \quad (58)$$

where $(\check{\mathbf{w}}_i^{t+1})_{\mathcal{D}_i^1}$ and $(\check{\mathbf{w}}_i^{t+1})_{\mathcal{D}_i^2}$ are the updated results based on dataset \mathcal{D}_i^1 and \mathcal{D}_i^2 . The first equality holds due to that ∇g_i is the only quantity in the update (15) which depends on the local dataset of client i , and the third equality holds due to that $\mathbf{z}_{i,n}^1, \mathbf{z}_{i,n}^2$ are the only two different records between two datasets. The first inequality holds since all $\mathbf{z}_{i,n}$ are non-negative. We next check how the added noise affect $\tilde{\mathbf{w}}_i^{t+1}$. Using (26), we have

$$\begin{aligned} \tilde{\mathbf{w}}_i^{t+1} &= \mathbf{w}_{i,\text{ex}}^{t,K_i^t-1} - \eta_w \left(\nabla g_i \left(\mathbf{w}_{i,\text{ex}}^{t,K_i^t-1} \right) \right. \\ &\quad \left. + \gamma_i \left(\mathbf{w}_{i,\text{ex}}^{t,K_i^t-1} - \mathbf{w}_{\text{con}}^t \right) \right) + \eta_w \mathbf{s}_i^t \\ &= \mathbf{w}_i^{t+1} + \eta_w \mathbf{s}_i^t \end{aligned} \quad (59)$$

According to [44], in one iteration, if the upload model updates is (ϵ, δ) -DP, the standard variance σ^* of the added Gaussian noise should satisfy $\sigma^* \geq \text{sensitivity} \cdot \sqrt{2 \ln(1.25/\delta)/\epsilon}$. Thus, for the t -th iteration of the i -th clients, if

$$\begin{aligned} \sigma_i^* &= \eta_w \sigma_i^t \geq \frac{2\sqrt{2 \ln(1.25/\delta_i^t)} \eta_w B_z}{N_i \epsilon_i^t} \\ \implies \sigma_i^t &\geq \frac{2\sqrt{2 \ln(1.25/\delta_i^t)} B_z}{N_i \epsilon_i^t} \end{aligned} \quad (60)$$

the publishing is $(\epsilon_i^t, \delta_i^t)$ -differentially private. Next, leveraging the Theorem 3.5 of [45], we conclude that the mechanism $M_i(\mathcal{S}_i)$ is $(\bar{\epsilon}_i, \bar{\delta}_i)$ -differential privacy.

REFERENCES

- [1] W. L. Hamilton, R. Ying, and J. Leskovec, "Representation learning on graphs: Methods and applications," *arXiv preprint arXiv:1709.05584*, 2017.
- [2] L. Stanković, M. Daković, and E. Sejdić, "Introduction to graph signal processing," in *Vertex-Frequency Analysis of Graph Signals*, pp. 3–108, Springer, 2019.
- [3] J. Friedman, T. Hastie, and R. Tibshirani, "Sparse inverse covariance estimation with the graphical lasso," *Biostatistics*, vol. 9, no. 3, pp. 432–441, 2008.
- [4] X. Dong, D. Thanou, M. Rabbat, and P. Frossard, "Learning graphs from data: A signal representation perspective," *IEEE Signal Processing Magazine*, vol. 36, no. 3, pp. 44–63, 2019.
- [5] Z. Wu, S. Pan, F. Chen, G. Long, C. Zhang, and S. Y. Philip, "A comprehensive survey on graph neural networks," *IEEE transactions on neural networks and learning systems*, vol. 32, no. 1, pp. 4–24, 2020.
- [6] G. Mateos, S. Segarra, A. G. Marques, and A. Ribeiro, "Connecting the dots: Identifying network structure via graph signal processing," *IEEE Signal Processing Magazine*, vol. 36, no. 3, pp. 16–43, 2019.
- [7] M. Yuan and Y. Lin, "Model selection and estimation in the gaussian graphical model," *Biometrika*, vol. 94, no. 1, pp. 19–35, 2007.
- [8] D. I. Shuman, S. K. Narang, P. Frossard, A. Ortega, and P. Vandergheynst, "The emerging field of signal processing on graphs: Extending high-dimensional data analysis to networks and other irregular domains," *IEEE signal processing magazine*, vol. 30, no. 3, pp. 83–98, 2013.
- [9] A. Ortega, P. Frossard, J. Kovačević, J. M. Moura, and P. Vandergheynst, "Graph signal processing: Overview, challenges, and applications," *Proceedings of the IEEE*, vol. 106, no. 5, pp. 808–828, 2018.
- [10] X. Dong, D. Thanou, P. Frossard, and P. Vandergheynst, "Learning laplacian matrix in smooth graph signal representations," *IEEE Transactions on Signal Processing*, vol. 64, no. 23, pp. 6160–6173, 2016.
- [11] V. Kalofolias, "How to learn a graph from smooth signals," in *Artificial Intelligence and Statistics*, pp. 920–929, PMLR, 2016.
- [12] P. Danaher, P. Wang, and D. M. Witten, "The joint graphical lasso for inverse covariance estimation across multiple classes," *Journal of the Royal Statistical Society: Series B (Statistical Methodology)*, vol. 76, no. 2, pp. 373–397, 2014.
- [13] F. Huang and S. Chen, "Joint learning of multiple sparse matrix gaussian graphical models," *IEEE transactions on neural networks and learning systems*, vol. 26, no. 11, pp. 2606–2620, 2015.
- [14] L. Gan, X. Yang, N. Narisetty, and F. Liang, "Bayesian joint estimation of multiple graphical models," *Advances in Neural Information Processing Systems*, vol. 32, 2019.
- [15] D. Hallac, Y. Park, S. Boyd, and J. Leskovec, "Network inference via the time-varying graphical lasso," in *Proceedings of the 23rd ACM SIGKDD International Conference on Knowledge Discovery and Data Mining*, pp. 205–213, 2017.
- [16] X. Yang, M. Sheng, Y. Yuan, and T. Q. Quek, "Network topology inference from heterogeneous incomplete graph signals," *IEEE Transactions on Signal Processing*, vol. 69, pp. 314–327, 2020.
- [17] S. Segarra, Y. Wang, C. Uhler, and A. G. Marques, "Joint inference of networks from stationary graph signals," in *2017 51st Asilomar Conference on Signals, Systems, and Computers*, pp. 975–979, IEEE, 2017.
- [18] M. Navarro, Y. Wang, A. G. Marques, C. Uhler, and S. Segarra, "Joint inference of multiple graphs from matrix polynomials," *arXiv preprint arXiv:2010.08120*, 2020.
- [19] K. Yamada, Y. Tanaka, and A. Ortega, "Time-varying graph learning with constraints on graph temporal variation," *arXiv preprint arXiv:2001.03346*, 2020.
- [20] V. Kalofolias, A. Loukas, D. Thanou, and P. Frossard, "Learning time varying graphs," in *2017 IEEE International Conference on Acoustics, Speech and Signal Processing (ICASSP)*, pp. 2826–2830, Ieee, 2017.
- [21] Y. Yuan, D. W. Soh, X. Yang, K. Guo, and T. Q. Quek, "Joint network topology inference via structured fusion regularization," *arXiv preprint arXiv:2103.03471*, 2021.
- [22] Y. Yuan, X. Yang, K. Guo, T. Q. Quek, et al., "GRACCE: Graph signal clustering and multiple graph estimation," *IEEE Transactions on Signal Processing*, vol. 70, pp. 2015–2030, 2022.
- [23] P. Kairouz, H. B. McMahan, B. Avent, A. Bellet, M. Bennis, A. N. Bhagoji, K. Bonawitz, Z. Charles, G. Cormode, R. Cummings, et al., "Advances and open problems in federated learning," *Foundations and Trends® in Machine Learning*, vol. 14, no. 1–2, pp. 1–210, 2021.
- [24] T. Li, A. K. Sahu, A. Talwalkar, and V. Smith, "Federated learning: Challenges, methods, and future directions," *IEEE Signal Processing Magazine*, vol. 37, no. 3, pp. 50–60, 2020.
- [25] T. Yang, X. Yi, J. Wu, Y. Yuan, D. Wu, Z. Meng, Y. Hong, H. Wang, Z. Lin, and K. H. Johansson, "A survey of distributed optimization," *Annual Reviews in Control*, vol. 47, pp. 278–305, 2019.
- [26] B. McMahan, E. Moore, D. Ramage, S. Hampson, and B. A. y Arcas, "Communication-efficient learning of deep networks from decentralized data," in *Artificial intelligence and statistics*, pp. 1273–1282, PMLR, 2017.
- [27] A. Z. Tan, H. Yu, L. Cui, and Q. Yang, "Towards personalized federated learning," *IEEE Transactions on Neural Networks and Learning Systems*, 2022.
- [28] Y. Mansour, M. Mohri, J. Ro, and A. T. Suresh, "Three approaches for personalization with applications to federated learning," *arXiv preprint arXiv:2002.10619*, 2020.
- [29] V. Smith, C.-K. Chiang, M. Sanjabi, and A. S. Talwalkar, "Federated multi-task learning," *Advances in neural information processing systems*, vol. 30, 2017.
- [30] A. Ghosh, J. Chung, D. Yin, and K. Ramchandran, "An efficient framework for clustered federated learning," *Advances in Neural Information Processing Systems*, vol. 33, pp. 19586–19597, 2020.
- [31] C. Finn, P. Abbeel, and S. Levine, "Model-agnostic meta-learning for fast adaptation of deep networks," in *International conference on machine learning*, pp. 1126–1135, PMLR, 2017.
- [32] H. B. McMahan, D. Ramage, K. Talwar, and L. Zhang, "Learning differentially private recurrent language models," *arXiv preprint arXiv:1710.06963*, 2017.
- [33] R. Xu, N. Baracaldo, and J. Joshi, "Privacy-preserving machine learning: Methods, challenges and directions," *arXiv preprint arXiv:2108.04417*, 2021.
- [34] E. De Cristofaro, "An overview of privacy in machine learning," *arXiv preprint arXiv:2005.08679*, 2020.
- [35] A. Bhowmick, J. Duchi, J. Freidiger, G. Kapoor, and R. Rogers, "Protection against reconstruction and its applications in private federated learning," *arXiv preprint arXiv:1812.00984*, 2018.
- [36] T. Zhu, G. Li, W. Zhou, and S. Y. Philip, "Differentially private data publishing and analysis: A survey," *IEEE Transactions on Knowledge and Data Engineering*, vol. 29, no. 8, pp. 1619–1638, 2017.
- [37] C. Dwork, "Differential privacy: A survey of results," in *International conference on theory and applications of models of computation*, pp. 1–19, Springer, 2008.
- [38] A. Karaaslanli, S. Saha, S. Aviyente, and T. Maiti, "Multiview graph learning for single-cell rna sequencing data," *bioRxiv*, 2021.
- [39] Z. Li, C. Tang, X. Liu, X. Zheng, W. Zhang, and E. Zhu, "Consensus graph learning for multi-view clustering," *IEEE Transactions on Multimedia*, vol. 24, pp. 2461–2472, 2021.
- [40] Z. Hu, F. Nie, W. Chang, S. Hao, R. Wang, and X. Li, "Multi-view spectral clustering via sparse graph learning," *Neurocomputing*, vol. 384, pp. 1–10, 2020.
- [41] F. Nie, J. Li, X. Li, et al., "Self-weighted multiview clustering with multiple graphs," in *IJCAI*, pp. 2564–2570, 2017.
- [42] J. Nocedal and S. Wright, *Numerical optimization*. Springer Science & Business Media, 2006.
- [43] C. Dwork, F. McSherry, K. Nissim, and A. Smith, "Calibrating noise to sensitivity in private data analysis," in *Theory of cryptography conference*, pp. 265–284, Springer, 2006.
- [44] C. Dwork, A. Roth, et al., "The algorithmic foundations of differential privacy," *Foundations and Trends® in Theoretical Computer Science*, vol. 9, no. 3–4, pp. 211–407, 2014.

- [45] P. Kairouz, S. Oh, and P. Viswanath, “The composition theorem for differential privacy,” in *International conference on machine learning*, pp. 1376–1385, PMLR, 2015.
- [46] M. Abadi, A. Chu, I. Goodfellow, H. B. McMahan, I. Mironov, K. Talwar, and L. Zhang, “Deep learning with differential privacy,” in *Proceedings of the 2016 ACM SIGSAC conference on computer and communications security*, pp. 308–318, 2016.
- [47] D. M. Powers, “Evaluation: from precision, recall and f-measure to roc, informedness, markedness and correlation,” *arXiv preprint arXiv:2010.16061*, 2020.
- [48] S. Fortunato, “Community detection in graphs,” *Physics reports*, vol. 486, no. 3-5, pp. 75–174, 2010.
- [49] J. Han, J. Pei, and M. Kamber, *Data mining: concepts and techniques*. Elsevier, 2011.
- [50] S. S. Saboksayr, G. Mateos, and M. Cetin, “Online discriminative graph learning from multi-class smooth signals,” *Signal Processing*, vol. 186, p. 108101, 2021.

Supplementary Material

The proof of Theorem 2: The proof is similar with that of Theorem. We first provide the following lemma.

Lemma 3. Suppose that Assumption 1-3 hold, for any client i , the updated \mathbf{w}_i^{t+1} satisfies that

$$\begin{aligned} f_i(\mathbf{w}_i^{t+1}, \mathbf{w}_{\text{con}}^t) &\leq f_i(\mathbf{w}_i^t, \mathbf{w}_{\text{con}}^t) - \frac{1}{2\eta_w} \|\mathbf{w}_i^{t+1} - \mathbf{w}_i^t\|_2^2 \\ &+ \frac{\xi^2}{2\eta_w} \|\mathbf{w}_i^t - \mathbf{w}_i^{t-1}\|_2^2 + \|\mathbf{s}_i^t\|_2 (\xi B_r + \eta_w (B_g + \|\mathbf{s}_i^t\|_2)) \end{aligned} \quad (61)$$

Proof: Similar with (43), we have

$$\begin{aligned} &f_i(\mathbf{w}_i^{t+1}, \mathbf{w}_{\text{con}}^t) \\ &\leq f_i(\mathbf{w}_i^t, \mathbf{w}_{\text{con}}^t) + \langle \nabla_{\mathbf{w}_i} f_i(\mathbf{w}_{i,\text{ex}}^t, \mathbf{w}_{\text{con}}^t), \mathbf{w}_i^{t+1} - \mathbf{w}_i^t \rangle \\ &+ \frac{1}{2\eta_w} \|\mathbf{w}_i^{t+1} - \mathbf{w}_{i,\text{ex}}^t\|_2^2 \\ &\leq f_i(\mathbf{w}_i^t, \mathbf{w}_{\text{con}}^t) + \left\langle \mathbf{s}_i^t + \frac{1}{\eta_w} (\mathbf{w}_i^{t+1} - \mathbf{w}_{i,\text{ex}}^t), \mathbf{w}_i^t - \mathbf{w}_i^{t+1} \right\rangle \\ &+ \frac{1}{2\eta_w} \|\mathbf{w}_i^{t+1} - \mathbf{w}_{i,\text{ex}}^t\|_2^2 \\ &\leq f_i(\mathbf{w}_i^t, \mathbf{w}_{\text{con}}^t) - \frac{1}{2\eta_w} \|\mathbf{w}_i^{t+1} - \mathbf{w}_i^t\|_2^2 + \|\mathbf{s}_i^t\|_2 \|\mathbf{w}_i^{t+1} - \mathbf{w}_i^t\|_2 \\ &+ \frac{1}{2\eta_w} \|\mathbf{w}_i^t - \mathbf{w}_{i,\text{ex}}^t\|_2^2 \\ &= f_i(\mathbf{w}_i^t, \mathbf{w}_{\text{con}}^t) + \|\mathbf{s}_i^t\|_2 \|\mathbf{w}_i^t - \mathbf{w}_{i,\text{ex}}^t + \mathbf{w}_{i,\text{ex}}^t - \mathbf{w}_i^{t+1}\|_2 \\ &- \frac{1}{2\eta_w} \|\mathbf{w}_i^{t+1} - \mathbf{w}_i^t\|_2^2 + \frac{\xi^2}{2\eta_w} \|\mathbf{w}_i^t - \mathbf{w}_i^{t-1}\|_2^2 \\ &\leq f_i(\mathbf{w}_i^t, \mathbf{w}_{\text{con}}^t) + \|\mathbf{s}_i^t\|_2 \left(\|\mathbf{w}_i^t - \mathbf{w}_{i,\text{ex}}^t\|_2 - \frac{1}{2\eta_w} \|\mathbf{w}_i^{t+1} - \mathbf{w}_i^t\|_2 \right. \\ &\quad \left. + \|\mathbf{w}_{i,\text{ex}}^t - \mathbf{w}_i^{t+1}\|_2 \right) + \frac{\xi^2}{2\eta_w} \|\mathbf{w}_i^t - \mathbf{w}_i^{t-1}\|_2^2 \\ &\leq f_i(\mathbf{w}_i^t, \mathbf{w}_{\text{con}}^t) - \frac{1}{2\eta_w} \|\mathbf{w}_i^{t+1} - \mathbf{w}_i^t\|_2^2 + \frac{\xi^2}{2\eta_w} \|\mathbf{w}_i^t - \mathbf{w}_i^{t-1}\|_2^2 \\ &\quad + \|\mathbf{s}_i^t\|_2 \left(\xi \|\mathbf{w}_i^t - \mathbf{w}_i^{t-1}\|_2 + \eta_w \|\nabla_{\mathbf{w}_i} \hat{f}(\mathbf{w}_{i,\text{ex}}^t, \mathbf{w}_{\text{con}}^t)\|_2 \right) \\ &= f_i(\mathbf{w}_i^t, \mathbf{w}_{\text{con}}^t) - \frac{1}{2\eta_w} \|\mathbf{w}_i^{t+1} - \mathbf{w}_i^t\|_2^2 + \|\mathbf{s}_i^t\|_2 \left(\xi \|\mathbf{w}_i^t - \mathbf{w}_i^{t-1}\|_2 \right. \\ &\quad \left. + \eta_w \|\nabla_{\mathbf{w}_i} f(\mathbf{w}_{i,\text{ex}}^t, \mathbf{w}_{\text{con}}^t) + \mathbf{s}_i^t\|_2 \right) + \frac{\xi^2}{2\eta_w} \|\mathbf{w}_i^t - \mathbf{w}_i^{t-1}\|_2^2 \\ &\leq f_i(\mathbf{w}_i^t, \mathbf{w}_{\text{con}}^t) - \frac{1}{2\eta_w} \|\mathbf{w}_i^{t+1} - \mathbf{w}_i^t\|_2^2 + \frac{\xi^2}{2\eta_w} \|\mathbf{w}_i^t - \mathbf{w}_i^{t-1}\|_2^2 \\ &\quad + \|\mathbf{s}_i^t\|_2 (\xi B_r + \eta_w (B_g + \|\mathbf{s}_i^t\|_2)), \end{aligned} \quad (62)$$

where the second inequality holds due to (26) and that the following first-order optimality condition holds for all $\tilde{\mathbf{w}}_i \in \mathcal{W}$.

$$\left\langle \nabla_{\mathbf{w}_i} f_i(\mathbf{w}_{i,\text{ex}}^t, \mathbf{w}_{\text{con}}^t) + \mathbf{s}_i^t + \frac{1}{\eta_w} (\mathbf{w}_i^{t+1} - \mathbf{w}_{i,\text{ex}}^t), \tilde{\mathbf{w}}_i - \mathbf{w}_i^{t+1} \right\rangle \quad (63)$$

The third inequality holds due to the same reason as that of proof of Theorem 1. The fifth inequality holds due to the update procedure of our algorithm and the non-expansiveness

of projection operator. The last inequality holds due to Assumption 2 and (39). Finally, we complete the proof. \blacksquare

We next define

$$\begin{aligned} \tilde{E}_{\mathbf{w}_i}^t &= \sum_{i=1}^I \mathbb{E} [f_i(\mathbf{w}_i^t, \mathbf{w}_{\text{con}}^t) - f_i(\mathbf{w}_i^{t+1}, \mathbf{w}_{\text{con}}^t)] \\ \tilde{E}_{\mathbf{w}_{\text{con}}}^t &= \sum_{i=1}^I \mathbb{E} [f_i(\mathbf{w}_i^{t+1}, \mathbf{w}_{\text{con}}^t) + \lambda \|\mathbf{w}_{\text{con}}^t\|_1 - f_i(\mathbf{w}_i^{t+1}, \mathbf{w}_{\text{con}}^{t+1}) \\ &\quad + \lambda \|\mathbf{w}_{\text{con}}^{t+1}\|_1] \\ \tilde{e}_{\mathbf{w}_i}^t &= \frac{1}{2\eta_w} \mathbb{E} [\|\mathbf{w}_i^{t+1} - \mathbf{w}_i^t\|_2^2] - \frac{\xi^2}{2\eta_w} \mathbb{E} [\|\mathbf{w}_i^t - \mathbf{w}_i^{t-1}\|_2^2] \\ \tilde{e}_{\mathbf{w}_{\text{con}}}^t &= \frac{\rho C_\gamma^t}{2} \mathbb{E} [\|\mathbf{w}_{\text{con}}^t - \mathbf{w}_{\text{con}}^{t+1}\|_2^2] \\ C_{\mathbf{w}_i}^t &= \mathbb{E} [\|\mathbf{s}_i^t\|_2 (\xi B_r + \eta_w (B_g + \|\mathbf{s}_i^t\|_2))] \end{aligned} \quad (64)$$

Following (53), we have

$$\begin{aligned} &\sum_{t=0}^{T-1} \sum_{i=1}^I \tilde{e}_{\mathbf{w}_i}^t + \tilde{e}_{\mathbf{w}_{\text{con}}}^t - C_{\mathbf{w}_i}^t \\ &\leq \sum_{t=0}^{T-1} \tilde{E}_{\mathbf{w}_i}^t + \tilde{E}_{\mathbf{w}_{\text{con}}}^t \\ &= \sum_{i=1}^I \mathbb{E} [f_i(\mathbf{w}_i^0, \mathbf{w}_{\text{con}}^0)] - \mathbb{E} [f_i(\mathbf{w}_i^T, \mathbf{w}_{\text{con}}^T)] + \lambda \mathbb{E} [\|\mathbf{w}_{\text{con}}^0\|_1] \\ &\quad - \lambda \mathbb{E} [\|\mathbf{w}_{\text{con}}^T\|_1] \\ &\leq \sum_{i=1}^I \mathbb{E} [f_i(\mathbf{w}_i^0, \mathbf{w}_{\text{con}}^0)] - f_i^{\min} + \lambda \mathbb{E} [\|\mathbf{w}_{\text{con}}^0 - \mathbf{w}_{\text{con}}^T\|_1] \\ &\leq \sum_{i=1}^I \mathbb{E} [f_i(\mathbf{w}_i^0, \mathbf{w}_{\text{con}}^0)] - f_i^{\min} + \lambda \sqrt{p} B_r \triangleq \Delta_3, \end{aligned} \quad (65)$$

Furthermore, following (54), we have

$$\sum_{t=0}^{T-1} e_{\mathbf{w}_i}^t = \sum_{t=0}^{T-1} \frac{1-\xi^2}{2\eta_w} \mathbb{E} [\|\mathbf{w}_i^t - \mathbf{w}_i^{t-1}\|_2^2]. \quad (66)$$

Furthermore, we can also reach that

$$\begin{aligned} &\sum_{t=0}^{T-1} \left(\sum_{i=1}^I \mathbb{E} [\|\mathbf{s}_i^t\|_2 (\xi B_r + \eta_w (B_g + \|\mathbf{s}_i^t\|_2))] \right) \\ &= \sum_{t=0}^{T-1} \left(\sum_{i=1}^I (\xi B_r + \eta_w B_g) \mathbb{E} [\|\mathbf{s}_i^t\|_2] \right) + \sum_{t=0}^{T-1} \left(\sum_{i=1}^I \mathbb{E} [\|\mathbf{s}_i^t\|_2^2] \right) \\ &= \sqrt{2p} (\xi B_r + \eta_w B_g) TI\sigma + 2pTI\sigma^2 \end{aligned} \quad (67)$$

Equipped with (65), (66) and (67), we reach that

$$\begin{aligned} &\frac{1}{T} \sum_{t=0}^{T-1} \sum_{i=1}^I \frac{1-\xi^2}{2\eta_w} \mathbb{E} [\|\mathbf{w}_i^t - \mathbf{w}_i^{t-1}\|_2^2] + \frac{1}{T} \sum_{t=0}^{T-1} \tilde{e}_{\mathbf{w}_{\text{con}}}^t \\ &\geq 0 \leq \frac{\Delta_3}{T} + \sqrt{2p} (\xi B_r + \eta_w B_g) I\sigma + 2pI\sigma^2. \end{aligned} \quad (68)$$

Therefore, we can easily conclude that

$$\frac{1}{T} \sum_{t=0}^{T-1} \sum_{i=1}^I \mathbb{E} [\|\mathbf{w}_i^t - \mathbf{w}_i^{t-1}\|_2^2]$$

$$\begin{aligned} &\leq \frac{2\eta_w\Delta_3}{(1-\xi^2)T} + \frac{2\sqrt{2p}\eta_wI\sigma(\xi B_r + \eta_w B_g) + 4pI\eta_w\sigma^2}{1-\xi^2} \\ &= \frac{C_1}{T} + \Delta_1 \end{aligned} \tag{69}$$

$$\begin{aligned} &\frac{1}{T} \sum_{t=0}^{T-1} \mathbb{E} [\|\mathbf{w}_{\text{con}}^t - \mathbf{w}_{\text{con}}^{t+1}\|_2^2] \\ &\leq \frac{2B_r\Delta_3}{\rho IT} + \frac{2\sqrt{2p}IB_r\sigma(\xi B_r + \eta_w B_g) + 4pIB_r\sigma^2}{\rho I} \\ &= \frac{C_2}{T} + \Delta_2. \end{aligned} \tag{70}$$

■